References

1 Krakow D, Robertson SP, King LM, et al: Mutations in the gene encoding filamin B disrupt vertebral segmentation, joint formation and skeletogenesis. Nature Genet 2004; 36:405–410.

2 Kozlowski K, Sillence D, Cortis-Jones R, et al: Boomerang dysplasia. Br J Radiol 1985;58: 369–371.

3 Nishimura G, Horiuchi T, Kim OH, et al: Atypical skeletal changes in otopalatodigital syndrome type II: phenotypic overlap among otopalatodigital syndrome type II, boomerang dysplasia, atelosteogenesis type I and type III, and lethal male phenotype of Melnick-Needles syndrome. Am J Med Genet 1997;73:132–138.

4 Farrington-Rock C, Firestein MH, Bicknell LS, et al: Mutations in two regions of FLNB result in atelosteogenesis I and III. Hum Mutat 2006;27:705–710.

5 Bicknell LS, Morgan T, Bonafe L, et al: Mutations in FLNB cause boomerang dysplasia. J Med Genet 2005;42:e43.

6 Bicknell LS, Farrington-Rock C, Shafeghati Y, et al: A molecular and clinical study of Larsen syndrome caused by mutations in FLNB. J Med Genet 2007;44:89–98.

7 Schultz C, Langer LO, Laxova R, et al: Atelosteogenesis type III: long term survival, prenatal diagnosis, and evidence for dominant transmission. Am J Med Genet 1999;83:28–42.

8 Cassart M: Suspected fetal skeletal malformations or bone disease: how to explore. Pediatr Radiol 2010;40:1046–1051.

9 Ulla M, Aiello H, Cobos MP, et al: Prenatal diagnosis of skeletal dysplasias: contribution of three-dimensional computed tomography. Fetal Diagn Ther 2011;29:238–247.

10 Sawyer GM, Clark AR, Robertson SP, et al: Disease-associated substitutions in the filamin B actin binding domain confer enhanced actin binding affinity in the absence of major structural disturbance: insights from the crystal structures of filamin B actin binding domains. J Mol Biol 2009;390:1030–1047.

RESEARCH LETTER

AMERICAN JOURNAL OF medical genetics PART A

Mosaic upd(7)mat in a Patient With Silver–Russell Syndrome

Tomoko Fuke-Sato,[1,2] Kazuki Yamazawa,[1] Kazuhiko Nakabayashi,[3] Keiko Matsubara,[1] Kentaro Matsuoka,[4] Tomonobu Hasegawa,[2] Kazushige Dobashi,[5] and Tsutomu Ogata[1,6]*

[1]Department of Molecular Endocrinology, National Research Institute for Child Health and Development, Tokyo, Japan

[2]Department of Pediatrics, Keio University School of Medicine, Tokyo, Japan

[3]Department of Maternal-Fetal Biology, National Research Institute for Child Health and Development, Tokyo, Japan

[4]Division of Pathology, National Medical Center for Children and Mothers, Tokyo, Japan

[5]Department of Pediatrics, Showa University School of Medicine, Tokyo, Japan

[6]Department of Pediatrics, Hamamatsu University School of Medicine, Hamamatsu, Japan

Received 10 March 2011; Accepted 9 November 2011

How to Cite this Article:
Fuke-Sato T, Yamazawa K, Nakabayashi K, Matsubara K, Matsuoka K, Hasegawa T, Dobashi K, Ogata T. 2011. Mosaic upd(7)mat in a patient with Silver–Russell syndrome. Am J Med Genet Part A 9999:1–4.

TO THE EDITOR:

Silver–Russell syndrome (SRS) is a congenital developmental disorder characterized by pre- and post-natal growth failure, relative macroc[illegible] triangular face, hemihypotrophy, and 5th finger clinodactyly [illegible]ssell, 1954; Silver et al., 1953]. Recent studies have shown that hypomethylation (epimutation) of the paternally derived differentially methylated region (DMR) in the upstream of *H19* (*H19*-DMR) on chromosome 11p15 and maternal uniparental disomy for chromosome 7 (upd(7)mat) account for ~45% and ~5–10% of SRS patients, respectively [Eggermann, 2010; Binder et al., 2011]. Furthermore, consistent with the involvement of imprinted genes in both body and placental growth [for review, Coan et al., 2005], epimutations of the *H19*-DMR and upd(7)mat are [illegible]n to result in placental hypoplasia [Yamazawa et al., 200[illegible] Here, we report on a Japanese boy with mosaic upd(7)mat)mat who was identified through genetic screenings in 120 patients with SRS-like phenotype.

This Japanese boy was conceived naturally to a 41-year-old father and a 36-year-old mother. The parents were non-consanguineous and healthy. The paternal height was 165 cm (−0.9 SD), and the maternal height 155 cm (−0.6 SD).

At 35 weeks of gestation, he was delivered by a cesarean because of fetal distress. At birth, his length was 37.4 cm (−3.1 SD), his weight 1.28 kg (−3.1 SD), and his head circumference 29.0 cm (−1.3 SD). The placenta weighed 400 g (−0.6 SD [Kagami et al., 2008]). Shortly after birth, he was found to have ventricular septal defect, hydronephrosis, and abnormal external genitalia (hypospadias, bifid scrotum, and bilateral cryptorchidism). He received orchidopexy at $1^{10}/_{12}$ years of age and genitoplasty at $2^{4}/_{12}$ years of age. He exhibited feeding difficulty and speech delay.

At $5^{1}/_{12}$ years of age, he was referred because of short stature. His height was 87.9 cm (−4.3 SD), weight was 10.4 kg (−2.9 SD), and his head circumference 49.0 cm (−0.7 SD). Physical examination showed relative macrocephaly, abnormal teeth, 5th finger clinodactyly, and underdeveloped muscles. There was no hemihypotrophy. Endocrine studies for short stature yielded normal results, as did radiological examinations. His karyotype was 46,XY in all the 50 lymphocytes examined. He was clinically diagnosed as having SRS, and molecular studies were performed after obtaining the approval from the Institutional Review Board Committee at National Center for Child Health and Development and the written informed consent from the parents.

We first performed methylation analysis of the *MEST*-DMR on chromosome 7q32.2 using leukocyte genomic DNA by the previously described methods [Yamazawa et al., 2008b], because this patient showed rela[illegible] mild SRS-phenotype with speech delay

Grant sponsor: Japan[Q1] Society for the Promotion of Science (JSPS); Grant number: 22249010; Grant sponsor: Ministry of Health, Labor and Welfare; Grant number: H21-005; Grant sponsor: Grant of National Center for Child Health and Development; Grant number: 23A-1.

*Correspondence to:
Tsutomu Ogata, M.D., Department of Pediatrics, Hamamatsu University School of Medicine, Hamamatsu 431-3192, Japan.
E-mail: tomogata@hama-med.ac.jp

Published online 00 Month 2011 in Wiley Online Library (wileyonlinelibrary.com).
DOI 10.1002/ajmg.a.34404

and feeding difficulty characteristic of upd(7)mat [Hitchins et al., 2001; Kotzot, 2008]. The methylation analysis showed a major peak for methylated clones and a minor peak for unmethylated clones in this patient (Fig. 1A). We also examined the *H19*-DMR and other multiple DMRs on various chromosomes by the bio-COBRA (combined bisulfite restriction analysis) method, as reported previously [Yamazawa et al., 2010]. The *GRB10*-DMR on chromosome 7p12.1 and the *PEG10*-DMR on chromosome 7q21.3 exhibited skewed methylation patterns consistent with the predominance of maternally derived clones, as did the *MEST*-DMR (Fig. 1B). By

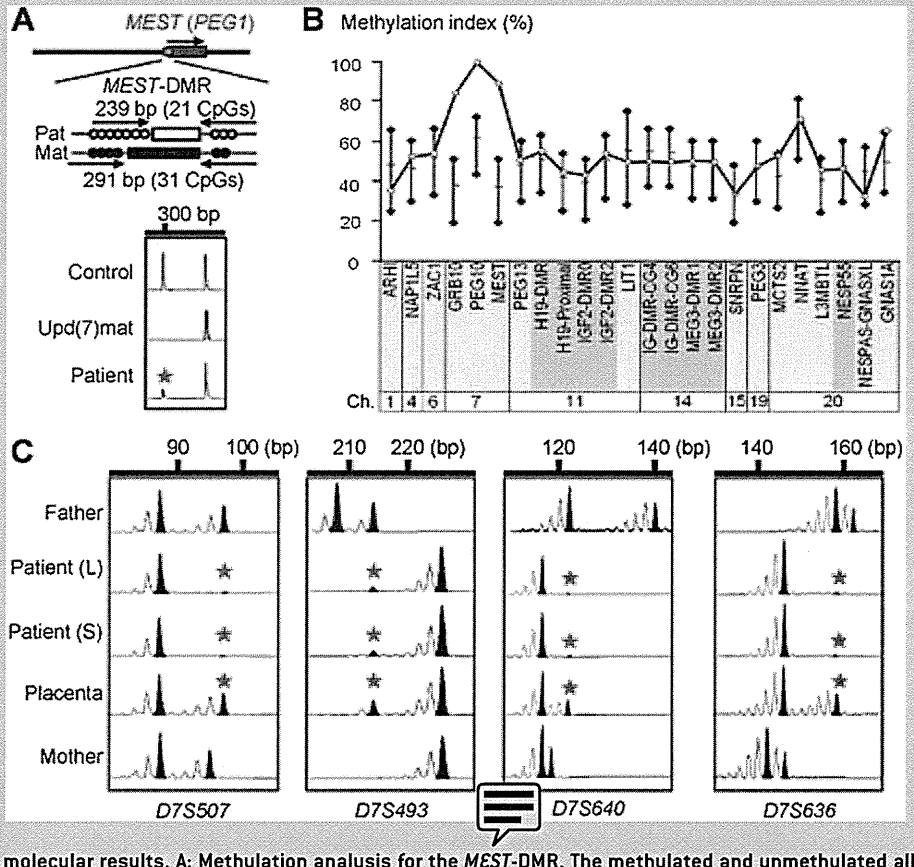

FIG. 1. Representative molecular results. A: Methylation analysis for the *MEST*-DMR. The methylated and unmethylated allele-specific primers were designed to yield PCR products of different sizes, and the PCR products were visualized on the 2100 Bioanalyzer (Agilent, Santa Clara, CA). Both methylated and unmethylated alleles are amplified in a control subject, and the methylated allele only is identified in a previously reported patient with upd(7)mat [Yamazawa et al., 2008b]. In this patient, a major peak for the methylated allele and a minor peak for the unmethylated allele (a red asterisk) are delineated. B: Methylation indices of 24 DMRs examined by the bio-COBRA. The PCR products were digested with methylation sensitive restriction enzymes, and the methylation indices (the ratios of methylated clones) were calculated using peak heights of digested and undigested fragments on the 2100 Bioanalyzer using 2100 expert software. The black vertical bars indicate the reference data in 20 normal control subjects (maximum − minimum). The DMRs highlighted in blue and pink are methylated after paternal and maternal transmissions, respectively.
C: Microsatellite analysis. Major peaks of maternal origin and minor peaks of paternal origin (red asterisks) are identified in this patient. The minor peaks of paternal origin are more obvious in the placenta than in the leukocytes (L) and salivary cells (S). Calculation of the mosaic ratio using the *D7S507* data, under the assumption of no trisomic cells. For this locus, the patient is considered to be heterozygous with the major 87 bp peak of maternal origin and a minor 97 bp peak of paternal origin. The father is also heterozygous with the two peaks of the same sizes, and the area under curve (AUC) is larger for the short 87 bp peak than for the long 97 bp peak. This unequal amplification is consistent with short products being more easily amplified than long products. In this patient, the AUC ratio between the major 87 bp peak and the minor 97 bp peak is obtained as 1.0:0.043 for leukocytes, 1.0:0.044 for salivary cells, and 1.0:0.803 in placental tissue, after compensation of the unequal amplification between the two peaks using the paternal data. Here, let "XL" represent the frequency of the upid(7)mat cells in leukocytes (thus, (1 − XL) denotes the frequency of normal cells in leukocytes). Then, the paternally derived 97 bp peak is generated by one paternally derived chromosome in the normal cells, that is, (1 − XL), and the maternally derived 87 bp peak is formed by the products from two maternally derived homologous chromosomes in the upid(7)mat cells and one maternally derived chromosome in the normal cells, that is, $\{2XL + (1 - XL)\} = (XL + 1)$. Thus, the AUC ratio between the two peaks is represented as $(XL + 1):(1 - XL) = 1.0:0.043$, and "XL" is calculated as 0.92 (92%). Similarly, when "XS" and "XP" represent the frequency of the upid(7)mat cells in salivary cells and placental tissue, respectively, "XS" is obtained as 0.91 (91%) and "XP" as 0.11 (11%). Furthermore, when "XB" represents the frequency of the upid(7)mat cells in buccal epithelium cells, "XB" is obtained as 0.91 (91%), on the basis of the previous report that salivary cells comprises ~40% of buccal epithelium cells and ~60% of leukocytes [Thiede et al., 2000].

TABLE I. The Results of Microsatellite Analysis

Locus	Position	Father	Patient (L)	Patient (S)	Placenta	Mother	Assessment
D7S517	7p22.2	254/258	(254)/258	(254)/258	(254)/258	256/258	Maternal Iso-D[a]/biparental
D7S507	7p15–21	87/97	87/(97)	87/(97)	87/(97)	87/95	Maternal Iso-D[a]/biparental
D7S493	7p15.3	208/214	(214)/226	(214)/226	(214)/226	226	Maternal D[b]/biparental
D7S484	7p14–15	96/100	(96)/98	(96)/98	(96)/98	98/100	Maternal Iso-D/biparental
D7S502	7q11.12	298	294/(298)	294/(298)	294/(298)	294/304	Maternal Iso-D/biparental
D7S669	7q11.2	116/126	(116)/124	(116)/124	(116)/124	124	Maternal D[b]/biparental
D7S515	7q21–22	169/173	171/(173)	171/(173)	171/(173)	169/171	Maternal Iso-D/biparental
D7S640	7q21.1–31.2	122/140	116/(122)	116/(122)	116/(122)	116/118	Maternal Iso-D/biparental
D7S684	7q34	169/179	177/(179)	177/(179)	177/(179)	177/179	Not informative
D7S636	7q35–36	158/162	146/(158)	146/(158)	146/(158)	142/146	Maternal Iso-D/biparental
D7S798	7q36	73/79	(79)/83	(79)/83	(79)/83	73/83	Maternal Iso-D/biparental

L, leukocytes; S, salivary cells; D, disomy.
The Arabic numbers denote the PCR product sizes in bp.
The minor peaks are indicated in parentheses.
[a]On the basis of the results of other informative loci, the major peaks are considered to be of maternal origin.
[b]Because of the maternal homozygosity, disomic status (isodisomy or heterodisomy) is unknown for these loci.

contrast, other DMRs including the *H19*-DMR showed normal methylation patterns.

We next performed microsatellite analysis for 11 loci on various parts of chromosome 7, using genomic DNA from leukocytes of the patient and the parents, from salivary cells of the patient, and from formalin-fixed and paraffin-embedded placental tissue. Major peaks consistent with maternal uniparental isodisomy and minor peaks of paternal origin were unequivocally identified for *D7S484, D7S502, D7S515, D7S640, D7S636*, and *D7S798*; furthermore, similar patterns were also detected for *D7S517, D7S507, D7S669*, and *D7S493*, although the results were not informative for *D7S684* (Fig. 1C and Table I). The minor peaks of paternal origin were similar between leukocytes and salivary cells and more evident in placental tissue. These findings, together with the normal karyotype in lymphocytes, indicated mosaic full maternal isodisomy for chromosome 7 (upid(7)mat) in this patient. Furthermore, since such a condition is frequently associated with mosaicism for trisomy 7 [Petit et al., 2011], we performed fluorescence in situ hybridization (FISH) analysis for stocked lymphocyte pellets, using a CEP7 probe for *D7Z1* (Abbott[Q3]). The FISH analysis identified two normal signals in 995 of 1,000 interphase nuclei examined, with no trace of trisomic nuclei; while a single signal was delineated in the remaining five nuclei, this was regarded as a false-positive finding. Thus, assuming no trisomic cells, the frequency of the full upid(7)mat cells was calculated as 92% in leukocytes, using the results of *D7S507* (Fig. 1C). In addition, similarly assuming no trisomic cells in other tissues, the frequency of the full upid(7)mat cells was calculated as 91% salivary cells (and in buccal cells) and 11% in placental tissue, although we could not perform FISH analysis in buccal cells and placental cells.

These results imply that this patient had an abnormal cell lineage with full upid(7)mat and a normal cell lineage with biparentally inherited chromosome 7 homologs at least in lymphocytes, and these had no trisomy 7. It is likely that mitotic non-disjunction and subsequent trisomy rescue (loss of the paternally derived chromosome 7 from a trisomic cell) took place in the post-zygotic developmental stage, resulting in the production of the mosaic full upid(7)mat (Fig. 2). While full upid(7)mat can also be produced by monosomy rescue (duplication of a single maternally derived chromosome 7 in a zygote), this mechanism is predicted to cause non-mosaic rather than mosaic upid(7)mat [Miozzo et al., 2001]. Although it remains to be clarified why trisomic cells mediating the production of full upid(7)mat cells were apparently absent in lymphocytes of this patient, there might be a negative selection against lymphocytes with trisomy 7.

However, the presence or absence of demonstrable trisomic cells was studied only in lymphocytes. In this regard, trisomic cells have been identified more frequently in skin fibroblasts and amniocytes than in blood cells in patients with mosaic trisomy 7 [Chen et al., 2010; Petit et al., 2011], and they are usually more frequently detected in the placental tissue than in the body tissue, as has been demonstrated by confined placental trisomy [Kalousek et al., 1991]. These findings would argue for the possible presence of trisomic cells in several tissues including placenta of this patient.

The full upid(7)mat cells were assessed to account for the majority of the leukocytes and salivary cells (buccal cells) and the minority of the placental tissue, under the assumption of no

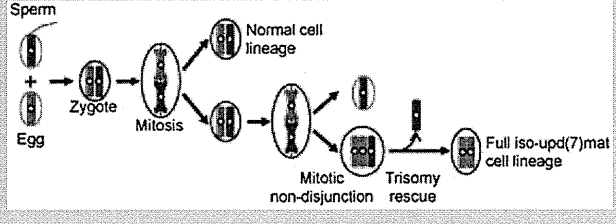

FIG. 2. Schematic representation of the generation of the mosaic upid(7)mat. The maternally and paternally derived chromosome 7 homologs are shown in red and blue, respectively. In this figure, mitotic non-disjunction is assumed at the second mitosis.

trisomic cells. In this regard, if trisomic cells may be present in a certain fraction of buccal cells and placental tissue, the full upid-(7)mat cells would still account for a relatively major fraction of buccal cells and a relatively minor fraction of the placental cells. While such a variation in the frequency of the full upid(7)mat cells among different tissues would primarily be a stochastic event, it should be pointed out that human genetic studies are usually performed for leukocytes. Indeed, if the upid(7)mat cells were barely present in leukocytes, the mosaic upid(7)mat would not have been detected. Such a bias in human studies would more or less be relevant to the relative predominance of the full upid(7)mat cells in leukocytes.

Two findings are noteworthy with regard to clinical features of this patient. First, this patient had relatively mild SRS phenotype with speech delay and feeding difficulty. Since such clinical features are grossly consistent with those of patients with upd(7)mat [Hitchins et al., 2001; Kotzot, 2008], it is inferred that the upid-(7)mat cells accounted for a considerable fraction of body cells relevant to the development of SRS phenotype. Second, the placental size remained within the normal range. This would be consistent with the relative paucity of the upid(7)mat cells in the placenta.

In summary, we observed mosaic upid(7)mat in a patient with SRS. Further studies will identify mosaic upd(7)mat with or without demonstrable trisomy 7 in patients with relatively mild SRS-like phenotype.

ACKNOWLEDGMENTS

This work was supported by the Grant-in-Aid for Scientific Research (A) (22249010) from the Japan Society for the Promotion of Science (JSPS), by the Grants for Health Research on Children, Youth, and Families (H21-005) from the Ministry of Health, Labor and Welfare, and by the Grant of National Center for Child Health and Development (23A-1).

REFERENCES

Binder G, Begemann M, Eggermann T, Kannenberg K. 2011. Silver-Russell syndrome. Best Pract Res Clin Endocrinol Metab 25:153–160.

Chen CP, Su YN, Chern SR, Hwu YM, Lin SP, Hsu CH, Tsai FJ, Wang TY, Wu PC, Lee CC, Chen YT, Chen LF, Wang W. 2010. Mosaic trisomy 7 at amniocentesis: Prenatal diagnosis and molecular genetic analyses. Taiwan J Obstet Gynecol 49:333–340.

Coan PM, Burton GJ, Ferguson-Smith AC. 2005. Imprinted genes in the placenta: A review. Placenta 26:S10–S20.

Eggermann T. 2010. Russell–Silver syndrome. Am J Med Genet Part C 154C:355–364.

Hitchins MP, Stanier P, Preece MA, Moore GE. 2001. Silver-Russell syndrome: A dissection of the genetic aetiology and candidate chromosomal regions. J Med Genet 38:810–819.

Kagami M, Yamazawa K, Matsubara K, Matsuo N, Ogata T. 2008. Placentomegaly in paternal uniparental disomy for human chromosome 14. Placenta 29:760–761.

Kalousek DK, Howard-Peebles PN, Olson SB, Barrett IJ, Dorfmann A, Black SH, Schulman JD, Wilson RD. 1991. Confirmation of CVS mosaicism in term placentae and high frequency of intrauterine growth retardation association with confined placental mosaicism. Prenat Diagn 11:743–750.

Kotzot D. 2008. Maternal uniparental disomy 7 and Silver–Russell syndrome—Clinical update and comparison with other subgroups. Eur J Med Genet 51:444–451.

Miozzo M, Grati FR, Bulfamante G, Rossella F, Cribiù M, Radaelli T, Cassani B, Persico T, Cetin I, Pardi G, Simoni G. 2011. Post-zygotic origin of complete maternal chromosome 7 isodisomy and consequent loss of placental *PEG1/MEST* expression. Placenta 22:813–821.

Petit F, Holder-Espinasse M, Duban-Bedu B, Bouquillon S, Boute-Benejean O, Bazin A, Rouland V, Manouvrier-Hanu S, Delobel B. 2011. Trisomy 7 mosaicism prenatally misdiagnosed and maternal uniparental disomy in a child with pigmentary mosaicism and Russell–Silver syndrome. Clin Genet [Epub ahead of print], PHID: 21204802.

Russell A. 1954. A syndrome of intra-uterine dwarfism recognizable at birth with cranio-facial dysostosis, disproportionately short arms and other anomalies. Proc R Soc Med 47:1040–1044.

Silver HK, Kiyasu W, George J, Deamer WC. 1953. Syndrome of congenital hemihypertrophy, shortness of stature, and elevated urinary gonadotrophins. Pediatrics 12:368–375.

Thiede C, Prange-Krex G, Freiberg-Richter J, Bornhäuser M, Ehninger G. 2000. Buccal swabs but not mouthwash samples can be used to obtain pretransplant DNA fingerprints from recipients of allogeneic bone marrow transplants. Bone Marrow Transplant 25:575–577.

Yamazawa K, Kagami M, Nagai T, Kondoh T, Onigata K, Maeyama K, Hasegawa T, Hasegawa Y, Yamazaki T, Mizuno S, Miyoshi Y, Miyagawa S, Horikawa R, Matsuoka K, Ogata T. 2008a. Molecular and clinical findings and their correlations in Silver-Russell syndrome: Implications for a positive role of IGF2 in growth determination and differential imprinting regulation of the *IGF2-H19* domain in bodies and placentas. J Mol Med 86:1171–1181.

Yamazawa K, Kagami M, Ogawa M, Horikawa R, Ogata T. 2008b. Placental hypoplasia in maternal uniparental disomy for chromosome 7. Am J Med Genet Part A 146A:514–516.

Yamazawa K, Nakabayashi K, Kagami M, Sato T, Saitoh S, Horikawa R, Hizuka N, Ogata T. 2010. Parthenogenetic chimaerism/mosaicism with a Silver-Russell syndrome-like phenotype. J Med Genet 47:782–785.

AUTHOR QUERY FORM

JOURNAL: AMERICAN JOURNAL OF MEDICAL GENETICS PART A
Article: ajma_34404

Dear Author,

During the copyediting of your paper, the following queries arose. Please respond to these by annotating your proofs with the necessary changes/additions.

- If you intend to annotate your proof electronically, please refer to the E-annotation guidelines.
- If you intend to annotate your proof by means of hard-copy mark-up, please refer to the proof mark-up symbols guidelines. If manually writing corrections on your proof and returning it as a scanned pdf via email, do not write too close to the edge of the paper. Please remember that illegible mark-ups may delay publication.

Whether you opt for hard-copy or electronic annotation of your proofs, we recommend that you provide additional clarification of answers to queries by entering your answers on the query sheet, in addition to the text mark-up.

Query No.	Query	Remark
Q1	Please check the grant sponsors.	
Q2	Please check the change made in the reference citation (Silver et al., 1953).	
Q3	Please give address information for this manufacturer: city, state (if applicable), and country.	
Q4	Please provide the volume number and page range.	

European Journal of Human Genetics (2012) 20, 928–932

www.nature.com/ejhg

EJHG Open

ARTICLE

Relative frequency of underlying genetic causes for the development of UPD(14)pat-like phenotype

Masayo Kagami[1], Fumiko Kato[1], Keiko Matsubara[1], Tomoko Sato[1], Gen Nishimura[2] and Tsutomu Ogata*[,1,3]

Paternal uniparental disomy 14 (UPD(14)pat) results in a unique constellation of clinical features, and a similar phenotypic constellation is also caused by microdeletions involving the *DLK1-MEG3* intergenic differentially methylated region (IG-DMR) and/or the *MEG3*-DMR and by epimutations (hypermethylations) affecting the DMRs. However, relative frequency of such underlying genetic causes remains to be clarified, as well as that of underlying mechanisms of UPD(14)pat, that is, trisomy rescue (TR), gamete complementation (GC), monosomy rescue (MR), and post-fertilization mitotic error (PE). To examine this matter, we sequentially performed methylation analysis, microsatellite analysis, fluorescence *in situ* hybridization, and array-based comparative genomic hybridization in 26 patients with UPD(14)pat-like phenotype. Consequently, we identified UPD(14)pat in 17 patients (65.4%), microdeletions of different patterns in 5 patients (19.2%), and epimutations in 4 patients (15.4%). Furthermore, UPD(14)pat was found to be generated through TR or GC in 5 patients (29.4%), MR or PE in 11 patients (64.7%), and PE in 1 patient (5.9%). Advanced maternal age at childbirth (≥35 years) was predominantly observed in the MR/PE subtype. The results imply that the relative frequency of underlying genetic causes for the development of UPD(14)pat-like phenotype is different from that of other imprinting disorders, and that advanced maternal age at childbirth as a predisposing factor for the generation of nullisomic oocytes through non-disjunction at meiosis 1 may be involved in the development of MR-mediated UPD(14)pat.
European Journal of Human Genetics (2012) **20,** 928–932; doi:10.1038/ejhg.2012.26; published online 22 February 2012

Keywords: genetic cause; maternal age effect; monosomy rescue; UPD(14)pat subtype

INTRODUCTION

Human chromosome 14q32.2 carries a ~1.2 Mb imprinted region with the germline-derived primary *DLK1-MEG3* intergenic differentially methylated region (IG-DMR) and the post-fertilization-derived secondary *MEG3*-DMR, together with multiple imprinted genes.[1,2] Both DMRs are methylated after paternal transmission and unmethylated after maternal transmission in the body, whereas in the placenta the IG-DMR alone remains as a DMR and the *MEG3*-DMR is rather hypomethylated irrespective of the parental origin.[2,3] Furthermore, it has been shown that the unmethylated IG-DMR and *MEG3*-DMR of maternal origin function as the imprinting centers in the placenta and the body, respectively, and that the IG-DMR acts as an upstream regulator for the methylation pattern of the *MEG3*-DMR in the body but not in the placenta.[3]

As a result of the presence of the imprinted region, paternal uniparental disomy 14 (UPD(14)pat) (OMIM #608149) causes a unique constellation of body and placental phenotypes such as characteristic face, bell-shaped small thorax, abdominal wall defect, polyhydramnios, and placentomegaly.[2,4,5] Furthermore, consistent with the essential role of the DMRs in the imprinting regulation, microdeletions and epimutations affecting the IG-DMR or both DMRs of maternal origin result in UPD(14)pat-like phenotype in both the body and the placenta, whereas a microdeletion involving the maternally inherited *MEG3*-DMR alone leads to UPD(14)pat-like phenotype in the body, but not in the placenta.[2,3]

Of the three underlying genetic causes for UPD(14)pat-like phenotype (UPD(14)pat, microdeletions, and epimutations), UPD(14)pat is primarily generated by four mechanisms, that is, trisomy rescue (TR), gamete complementation (GC), monosomy rescue (MR), and post-fertilization mitotic error (PE).[6] TR refers to a condition in which chromosome 14 of maternal origin is lost from a zygote with trisomy 14 formed by fertilization between a disomic sperm and a normal oocyte. GC results from fertilization of a disomic sperm with a nullisomic oocyte. MR refers to a condition in which chromosome 14 of paternal origin is replicated in a zygote with monosomy 14 formed by fertilization between a normal sperm and a nullisomic oocyte. PE is an event after formation of a normal zygote. In this regard, a nullisomic oocyte specific to GC and MR is produced by non-disjunction at meiosis 1 (M1) or meiosis 2 (M2), and non-disjunction at M1 is known to increase with maternal age, probably because of a long-term (10–50 years) meiotic arrest at prophase 1.[7]

However, relative frequency of the genetic causes for UPD(14)pat-like phenotype remains to be determined, as well as that of underlying mechanisms for the generation of UPD(14)pat. Here, we report our data on this matter, and discuss the difference in the relative frequency

[1]Department of Molecular Endocrinology, National Research Institute for Child Health and Development, Tokyo, Japan; [2]Department of Radiology, Tokyo Metropolitan Children's Medical Center, Fuchu, Japan; [3]Department of Pediatrics, Hamamatsu University School of Medicine, Hamamatsu, Japan
*Correspondence: Professor T Ogata, Department of Pediatrics, Hamamatsu University School of Medicine, Hamamatsu 431-3192, Japan. Tel: +81 53 435 2310; Fax: +81 53 435 2312; E-mail: tomogata@hama-med.ac.jp
Received 23 May 2011; revised 10 November 2011; accepted 26 December 2011; published online 22 February 2012

among imprinted disorders and the possible maternal age effect on the relative frequency.

PATIENTS AND METHODS

Patients

This study comprised 26 patients with UPD(14)pat-like phenotype (9 male patients and 17 female patients) (Table 1). Of the 26 patients, 18 patients have been reported previously; they consisted of nine sporadic patients with full UPD(14)pat,[4,5] one sporadic patient with segmental UPD(14)pat,[4] the proband of sibling cases and four sporadic patients with different patterns of microdeletions involving the unmethylated DMRs of maternal origin,[2,3] and three patients with epimutations (hypermethylations) of the two normally unmethylated DMRs of maternal origin.[2] The remaining eight patients were new sporadic cases.

Phenotypic findings of the 26 patients are summarized in Supplementary Table 1; detailed clinical features of patients 6 and 16–25 are as described previously,[2–4] and those of the eight new patients 3, 5, 10–14, and 26 are shown in Supplementary Table 2, together with those of patients 1, 2, 4, 7–9, and 15 in whom detailed phenotypes were not described in the previous report.[5] All the 26 patients were identified shortly after birth because of the unique bell-shaped thorax with coat-hanger appearance of the ribs on roentgenograms obtained because of asphyxia. Subsequent clinical analysis revealed that 25 of the 26 patients exhibited both body and placental UPD(14)pat-like phenotype, whereas the remaining one previously reported patient (patient 22) manifested body, but not placental, UPD(14)pat-like phenotype.[3] The karyotype was found to be normal in 25 patients, although cytogenetic analysis was not performed in one previously reported patient who died of respiratory failure at 2 h of age (patient 6).[4] One patient (patient 15) was conceived by *in vitro* fertilization-embryo transfer.[5] This study was approved by the Institute Review Board Committee at the National Center for Child Health and Development, and performed after obtaining written informed consent.

Analysis of underlying genetic causes in patients with UPD(14)pat-like phenotype

We sequentially performed methylation analysis, microsatellite analysis, and fluorescence *in situ* hybridization (FISH), using leukocyte genomic DNA samples and lymphocyte metaphase spreads of all the 26 patients with UPD(14)pat-like phenotype. The detailed methods were as reported previously.[2,3] In brief, methylation analysis was performed for the IG-DMR (CG4 and CG6) and the *MEG3*-DMR (CG7 and the CTCF-biding sites C and D) by combined bisulfite restriction analysis and bisulfite sequencing. Microsatellite analysis was performed for multiple loci on chromosome 14, by determining the sizes of PCR products obtained with fluorescently labeled forward primers and unlabeled reverse primers. FISH analysis was carried out for the IG-DMR and the *MEG3*-DMR using 5104-bp and 5182-bp long PCR products, respectively, together with the RP11-566I2 probe for 14q12 utilized as an internal control.

In this study, furthermore, oligonucleotide array-based comparative genomic hybridization (CGH) was also performed for the imprinted region of non-UPD(14)pat patients, using a custom-build oligo-microarray containing 12 600 probes for 14q32.2–q32.3 encompassing the imprinted region and ~10 000 reference probes for other chromosomal region (4×180K format, Design ID 032112) (Agilent Technologies, Palo Alto, CA, USA). The procedure was as described in the manufacturer's instructions.

Analysis of subtypes in patients with UPD(14)pat

UPD(14)pat subtype was determined by microsatellite analysis.[8,9] In brief, heterodisomy for at least one locus was regarded as indicative of TR- or GC-mediated UPD(14)pat (TR/GC subtype), whereas isodisomy for all the informative microsatellite loci was interpreted as indicative of MR- or PE-mediated UPD(14)pat (MR/PE subtype) (for details, see Supplementary Figure S1). Here, while heterodisomy and isodisomy for a pericentromeric region in the TR/GC subtype imply a disomic sperm generation through M1

Table 1 Summary of patients examined in this study

Patient	*Genetic cause*	*UPD(14)pat subtype*	*Maternal age at childbirth (years)*	*Paternal age at childbirth (years)*	*Remark*	*Reference*
1	UPD(14)pat	TR/GC [M1]	31	35		5
2	UPD(14)pat	TR/GC [M1]	28	29		5
3	UPD(14)pat	TR/GC [M1]	29	38		This report
4	UPD(14)pat	TR/GC [M1]	36	41		5
5	UPD(14)pat	TR/GC [M2]	30	30		This report
6	UPD(14)pat	MR/PE	42	Unknown		4,5
7	UPD(14)pat	MR/PE	31	28		5
8	UPD(14)pat	MR/PE	32	33		5
9	UPD(14)pat	MR/PE	26	35		5
10	UPD(14)pat	MR/PE	38	38		This report
11	UPD(14)pat	MR/PE	26	32		This report
12	UPD(14)pat	MR/PE	41	36		This report
13	UPD(14)pat	MR/PE	30	28		This report
14	UPD(14)pat	MR/PE	39	34		This report
15	UPD(14)pat	MR/PE	42	37	Born after IVF-ET	5
16	UPD(14)pat	MR/PE	36	36		4,5
17	UPD(14)pat-seg.	PE	27	24	Segmental isodisomy	4,5
18	Microdeletion		31	34		2
19	Microdeletion		33	36		2
20	Microdeletion		28	27		2
21	Microdeletion		27	37	IG-DMR alone	3
22	Microdeletion		25	25	*MEG3*-DMR alone	3
23	Epimutation		35	36		2
24	Epimutation		28	26		2
25	Epimutation		27	30		2
26	Epimutation		33	33		This report

Abbreviation: IVF-ET, *in vivo* fertilization-embryo transfer using parental gametes.
The microdeletions in patients 18–22 are different in size.

and M2 non-disjunction respectively,[9] such discrimination between M1 and M2 non-disjunctions is impossible for the development of a nullisomic oocyte. Furthermore, it is usually impossible to discriminate between TR and GC, although the presence of trisomic cells is specific to TR. Similarly, it is also usually impossible to discriminate between MR and PE, although identification of segmental isodisomy or mosaicism is unique to PE (PE subtype).

Analysis of parental ages

We examined parental ages at childbirth in patients of different underlying causes and different UPD(14)pat subtypes. Statistical significance of the relative frequency was examined by the Fisher's exact probability test, and that of the median age by the Mann–Whitney's *U*-test. $P<0.05$ was considered significant.

RESULTS

Analysis of underlying causes in patients with UPD(14)pat-like phenotype

For the eight new sporadic patients, methylation analysis invariably revealed hypermethylation of both DMRs, and microsatellite analysis showed UPD(14)pat in seven patients and biparentally inherited homologs of chromosome 14 in the remaining one patient (patient 26). FISH analysis for patient 26 identified two signals for the two DMRs, and subsequently performed array CGH analysis showed no evidence for genomic rearrangements (Supplementary Figure S2). Thus, patient 26 was assessed to have an epimutation affecting the two DMRs. Furthermore, the results of array CGH analysis confirmed the presence of microdeletions in patients 18–21 and the absence of a discernible microdeletion in patients 23–25 (Supplementary Figure S2) (array CGH analysis was not performed in patient 22 with a 4303-bp microdeletion[3] because of the lack of DNA sample available). Thus, together with our previous data, all the 26 patients with UPD(14)pat-like phenotype had genetic alteration involving the imprinted region on chromosome14q32.2.

Consequently, the 26 patients with UPD(14)pat-like phenotype were classified as follows: (1) 16 sporadic patients with full UPD(14)pat and 1 sporadic patient with segmental UPD(14)pat (UPD(14)pat group); (2) the proband of the sibling cases and two sporadic patients with different patterns of microdeletions involving the two DMRs, one sporadic patient with a microdeletion involving the IG-DMR alone in whom the *MEG3*-DMR was epimutated, and one patient with a microdeletion involving the *MEG3*-DMR alone (deletion group); and (3) four patients with epimutations (hypermethylations) of both DMRs (epimutation group) (Figure 1 and Table 1).

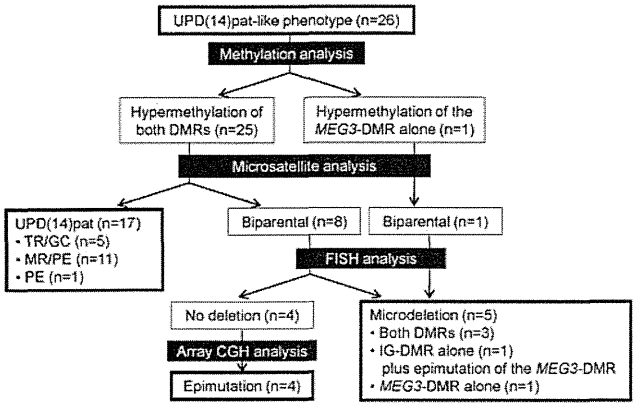

Figure 1 Classification of 26 patients with UPD(14)pat-like phenotype.

Analysis of subtypes in patients with UPD(14)pat

Heterozygosity for at least one locus indicative of TR/GC subtype was identified in five patients (patients 1–5), and the disomic pattern of pericentromeric region indicated M1 non-disjunction in patients 1–4 and M2 non-disjunction in patient 5. Full isodisomy consistent with MR/PE subtype was detected in 11 patients (patients 6–16), and segmental isodisomy unique to PE subtype was revealed in 1 patient (patient 17) (Table 1, Figure 1, and Supplementary Figure S3).

Analysis of parental ages

The distribution of parental ages at childbirth is shown in Figure 2. The advanced maternal age at childbirth ($\geq$35 years) was predominantly observed in the MR/PE subtype of UPD(14)pat. Furthermore, while the relative frequency of aged mothers ($\geq$35 years) did not show a significant difference between the MR/PE subtype of UPD(14)pat (6/11) and (i) other subtypes of UPD(14)pat (1/6) (P=0.159), (ii) deletion group (0/5) (P=0.057), and (iii) epimutation group (1/4) (P=0.338), it was significantly different between the MR/PE subtype and the sum of other subtypes of UPD(14)pat, deletion group, and epimutation group (2/15) (P=0.034). Similarly, while the median maternal age did not show a significant difference between the MR/PE subtype of UPD(14)pat (36 years) *vs* (i) other subtypes of UPD(14)pat (29.5 years) (P=0.118), (ii) deletion type (28 years) (P=0.088), and (iii) epimutation type (30.5 years) (P=0.295), it was significantly different between the MR/PE subtype of UPD(14)pat and the sum of other subtypes of UPD(14)pat, deletion group, and epimutation group (29 years) (P=0.045).

The paternal ages were similar irrespective of the genetic causes and the UPD(14)pat subtypes. In addition, the median paternal age was comparable between the TR/GC subtype of UPD(14)pat that postulates the production of a disomic sperm (35.0 years) and the sum of other subtypes of UPD(14)pat, deletion group, and epimutation group that assumes the production of a normal sperm (33.5 years) (P=0.322).

DISCUSSION

This study revealed that the UPD(14)pat-like phenotype was caused by UPD(14)pat in 65.4% of patients, by microdeletions in 19.2% of patients, and by epimutations in 15.4% of patients. Although the relative frequency of underlying genetic factors for the development of UPD(14)pat-like phenotype has been reported previously,[10] most data are derived from our previous publications. Thus, the present results are regarded as the updated and extended data on the relative frequency. For the relative frequency, it is notable that 25 of the 26 patients were confirmed to have normal karyotype, although chromosome analysis was not performed in patient 6. Thus, while Robertsonian translocations involving chromosome 14 is known to be a

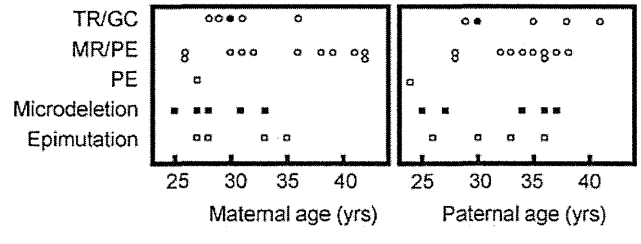

Figure 2 The distribution of parental ages at childbirth according to the underlying genetic causes for the development of UPD(14)pat-like phenotype and UPD(14)pat subtypes. Of the five plots for the TR/GC subtype, open and black circles indicate the TR/GC subtype due to non-disjunction at paternal M1 and M2, respectively.

predisposing factor for the occurrence of UPD(14)pat,[11–16] such a possible chromosomal effect has been excluded in nearly all patients examined in this study.

The relative frequency of underlying causes has also been reported in other imprinting disorders.[8,17–19] The data are summarized in Table 2 (a similar summary has also been reported recently by Hoffmann *et al*).[10] In particular, the results in patients with normal karyotype are available in Prader–Willi syndrome (PWS).[8] Furthermore, PWS is also known to be caused by UPD, microdeletions, and epimutations affecting a single imprinting region,[8,19] although Silver–Russell syndrome and Beckwith–Wiedemann syndrome (BWS) can result from perturbation of at least two imprinted regions,[17,18] and BWS and Angelman syndrome can occur as a single gene disorder.[17,19] Thus, it is notable that the relative frequency of underlying causes is quite different between patients with UPD(14)pat-like phenotype and those with PWS.[8,19] This would primarily be due to the presence of low copy repeats flanking the imprinted region on chromosome 15, because chromosomal deletions are prone to occur in regions harboring such repeat sequences.[20] Indeed, two types of microdeletions mediated by such low copy repeats account for a vast majority of microdeletions in patients with PWS,[21] whereas the microdeletions identified in patients with UPD(14)pat-like phenotype are different to each other. This would explain why microdeletions are less frequent and UPD and epimutations are more frequent in patients with UPD(14)pat-like phenotype than in those with PWS.

Advanced maternal age at childbirth was predominantly observed in the MR/PE subtype. This may imply the relevance of advanced maternal age to the development of MR-mediated UPD(14)pat, because the generation of nullisomic oocytes through M1 non-disjunction is a maternal age-dependent phenomenon.[22] Although no paternal age effect was observed, this is consistent with the previous data indicating no association of advanced paternal age with a meiotic error.[23] For the maternal age effect, however, several matters should be pointed out: (1) the number of analyzed patients is small, although it is very difficult to collect a large number of patients in this extremely rare disorder; (2) of the MR/PE subtype, the advanced maternal age is a risk factor for the generation of MR-mediated UPD(14)pat, but not for the development of PE-mediated UPD(14)pat; (3) it is impossible to discriminate between maternal age-dependent M1 non-disjunction and maternal age-independent M2 non-disjunction in the MR and GC subtypes (however, GC must be extremely rare, because it requires the concomitant occurrence of a nullisomic oocyte and a disomic sperm); (4) of the TR/GC subtype, the advanced maternal age is a risk factor for the generation of GC-mediated UPD(14)pat, but not for the development of TR-mediated UPD(14)pat; and (5) if a cryptic recombination(s) might remain undetected in some patients with apparently full isodisomy, this argues that such patients actually have TR- or GC-mediated UPD(14)pat rather than MR- or PE-mediated UPD(14)pat. Thus, further studies are required to examine the maternal age effect on the generation of MR-mediated UPD(14)pat. In addition, while a relationship is unlikely to exist between advanced maternal age and microdeletions and epimutations, this notion would also await further investigations.

Such a maternal age effect is also expected in the TR/GC subtype maternal UPDs after M1 non-disjunction, because the generation of disomic oocytes through M1 non-disjunction is also a maternal age-dependent phenomenon.[7] Indeed, such a maternal age effect has been shown for PWS patients with normal karyotype; the maternal age at childbirth was significantly higher in patients with heterodisomy for a very pericentromeric region indicative of TR/GC subtype UPD(15)mat after M1 non-disjunction than in those with other genetic causes.[8,9] For various chromosomes other than chromosome 15, furthermore, since maternal age at childbirth is higher in patients with maternal heterodisomy than in those with maternal isodisomy,[24] this would also argue for maternal age effect on the development of maternal UPDs. However, in the previous studies on maternal UPDs other than UPD(15)mat, the available data are quite insufficient to assess the maternal age effect. For example, although a relatively large number of patients with UPD(14)mat phenotype have been reported in the literature (reviewed in reference Hoffmann *et al*),[10] we could identify only six UPD(14)mat patients with normal karyotype in whom maternal age at childbirth was documented and microsatellite analysis was performed.[25–30] Furthermore, the microsatellite data are insufficient to identify the subtype of UPD(14)mat and to distinguish between M1 and M2 non-disjunction in the TR/GC subtype. Thus, while the maternal age at childbirth may be advanced in five patients with apparently TR/GC-mediated UPD(14)mat (27, 35, 37, 41, and 44 years)[25–27,29,30] (the maternal age at childbirth in the remaining one

Table 2 Relative frequency of genetic mechanisms in imprinting disorders

	UPD(14)pat-like phenotype	*BWS*	*SRS*	*AS*	*PWS*
Uniparental disomy	65.4%	16%	10%	3–5%	25% (25%)
	UPD(14)pat	UPD(11)pat (mosaic)	UPD(7)mat	UPD(15)pat	UPD(15)mat
Cryptic deletion	19.2%	Rare	—	70%	70% (72%)
Cryptic duplication	—	—	Rare	—	—
Epimutation					
Hypermethylation	15.4%	9%	—	—	2–5% (2%)
Affected DMR	IG-DMR/*MEG3*-DMR	*H19*-DMR	—	—	*SNRPN*-DMR
Hypomethylation	—	44%	>38%	2–5%	—
Affected DMR		KvDMR1	*H19*-DMR	*SNRPN*-DMR	
Gene mutation	—	5%	—	10-15%	—
Mutated gene		*CDKN1C*		*UBE3A*	
Unknown		25%	>40%	10%	
Reference	This study	17	18	19	8, 19

Abbreviations: AS, Angelman syndrome; BWS, Beckwith–Wiedemann syndrome; PWS, Prader–Willi syndrome; SRS, Silver–Russell syndrome.
Patients with abnormal karyotypes are included in BWS and AS, and not included in SRS. In PWS, the data including patients with abnormal karyotypes are shown, and those from patients with normal karyotype alone are depicted in parentheses.

patient with apparently MR/PE-mediated UPD(14)mat is 40 years),[28] the notion of a maternal age effect awaits further investigations for UPD(14)mat.

Finally, it appears to be worth pointing out that methylation analysis invariably revealed hypermethylated DMR(s) in all the 26 patients who were initially ascertained because of bell-shaped thorax with coat-hanger appearance of the ribs. This indicates that methylation analysis of the DMRs can be utilized for a screening of this condition, and that the constellation of clinical features in the UPD(14)pat-like phenotype, especially the bell-shaped thorax with coat-hanger appearance of the ribs, is highly unique to patients with UPD(14)pat-like phenotype.

In summary, this study confirms the relative frequency of underlying genetic causes for the UPD(14)pat phenotype and reveals the relative frequency of UPD(14)pat subtypes. Furthermore, the results emphasize the difference in the relative frequency of underlying genetic causes among imprinted disorders, and may support a possible maternal age effect on the generation of the nullisomic oocyte mediated UPD(14)pat. Further studies will permit a more precise assessment on these matters.

CONFLICT OF INTEREST

The authors declare no conflict of interest.

ACKNOWLEDGEMENTS

We thank Drs Kenji Kurosawa, Michiko Hayashidani, Toshio Takeuchi, Shinya Tanaka, Mika Noguch, Kouji Masumoto, Takeshi Utsunomiya, Yumiko Komatsu, Hirofumi Ohashi, Maureen J O'Sullivan, Andrew J Green, Yoshiyuki Watabe, Tsuyako Iwai, Hitoshi Kawato, Miho Torikai, Akiko Yamamoto, Nobuhiro Suzumori, Makoto Kuwajima, Hiroshi Yoshihashi, Yoriko Watanabe, and Jin Nishimura for material sampling and phenotype assessment. This work was supported by Grants for Research on Intractable Diseases (H22-161) and for Health Research on Children, Youth and Families (H21-005) from the Ministry of Health, Labor and Welfare, by Grants-in-Aid for Scientific Research (A) (22249010) and (B) (21028026) from the Japan Society for the Promotion of Science (JSPS), by Grants from Takeda Science Foundation and from Kanehara Foundation, and by the Grant for National Center for Child Health and Development (23A-1).

1 da Rocha ST, Edwards CA, Ito M, Ogata T, Ferguson-Smith AC: Genomic imprinting at the mammalian Dlk1-Dio3 domain. *Trends Genet* 2008; **24**: 306–316.
2 Kagami M, Sekita Y, Nishimura G *et al*: Deletions and epimutations affecting the human 14q32.2 imprinted region in individuals with paternal and maternal upd(14)-like phenotypes. *Nat Genet* 2008; **40**: 237–242.
3 Kagami M, O'Sullivan MJ, Green AJ *et al*: The IG-DMR and the MEG3-DMR at human chromosome 14q32.2: hierarchical interaction and distinct functional properties as imprinting control centers. *PLoS Genet* 2010; **6**: e1000992.
4 Kagami M, Nishimura G, Okuyama T *et al*: Segmental and full paternal isodisomy for chromosome 14 in three patients: narrowing the critical region and implication for the clinical features. *Am J Med Genet A* 2005; **138A**: 127–132.
5 Kagami M, Yamazawa K, Matsubara K, Matsuo N, Ogata T: Placentomegaly in paternal uniparental disomy for human chromosome 14. *Placenta* 2008; **29**: 760–761.
6 Shaffer LG, Agan N, Goldberg JD, Ledbetter DH, Longshore JW, Cassidy SB: American College of Medical Genetics statement of diagnostic testing for uniparental disomy. *Genet Med* 2001; **3**: 206–211.
7 Jones KT: Meiosis in oocytes: predisposition to aneuploidy and its increased incidence with age. *Hum Reprod Update* 2008; **14**: 143–158.
8 Matsubara K, Murakami N, Nagai T, Ogata T: Maternal age effect on the development of Prader-Willi syndrome resulting from upd(15)mat through meiosis 1 errors. *J Hum Genet* 2011; **56**: 566–571.
9 Robinson WP, Christian SL, Kuchinka BD *et al*: Somatic segregation errors predominantly contribute to the gain or loss of a paternal chromosome leading to uniparental disomy for chromosome 15. *Clin Genet* 2000; **57**: 349–358.
10 Hoffmann K, Heller R: Uniparental disomies 7 and 14. *Best Pract Res Clin Endocrinol Metab* 2011; **25**: 77–100.
11 Wang JC, Passage MB, Yen PH, Shapiro LJ, Mohandas TK: Uniparental heterodisomy for chromosome 14 in a phenotypically abnormal familial balanced 13/14 Robertsonian translocation carrier. *Am J Hum Genet* 1991; **48**: 1069–1074.
12 Papenhausen PR, Mueller OT, Johnson VP, Sutcliffe M, Diamond TM, Kousseff BG: Uniparental isodisomy of chromosome 14 in two cases: an abnormal child and a normal adult. *Am J Med Genet* 1995; **59**: 271–275.
13 Cotter PD, Kaffe S, McCurdy LD, Jhaveri M, Willner JP, Hirschhorn K: Paternal uniparental disomy for chromosome 14: a case report and review. *Am J Med Genet* 1997; **70**: 74–79.
14 Yano S, Li L, Owen S, Wu S, Tran T: A further delineation of the paternal uniparental disomy (UPD14): the fifth reported liveborn case. *Am J Hum Genet* 2001; **69** (Suppl): A739.
15 Kurosawa K, Sasaki H, Sato Y *et al*: Paternal UPD14 is responsible for a distinctive malformation complex. *Am J Med Genet A* 2002; **110**: 268–272.
16 McGowan KD, Weiser JJ, Horwitz J *et al*: The importance of investigating for uniparental disomy in prenatally identified balanced acrocentric rearrangements. *Prenat Diagn* 2002; **22**: 141–143.
17 Sasaki K, Soejima H, Higashimoto K *et al*: Japanese and North American/European patients with Beckwith-Wiedemann syndrome have different frequencies of some epigenetic and genetic alterations. *Eur J Hum Genet* 2007; **15**: 1205–1210.
18 Eggermann T: Epigenetic regulation of growth: lessons from Silver-Russell syndrome. *Endocr Dev* 2009; **14**: 10–19.
19 Gurrieri F, Accadia M: Genetic imprinting: the paradigm of Prader-Willi and Angelman syndromes. *Endocr Dev* 2009; **14**: 20–28.
20 Pujana MA, Nadal M, Guitart M, Armengol L, Gratacos M, Estivill X: Human chromosome 15q11-q14 regions of rearrangements contain clusters of LCR15 duplicons. *Eur J Hum Genet* 2002; **10**: 26–35.
21 Varela MC, Kok F, Setian N, Kim CA, Koiffmann CP: Impact of molecular mechanisms, including deletion size, on Prader-Willi syndrome phenotype: study of 75 patients. *Clin Genet* 2005; **67**: 47–52.
22 Pellestor F, Andreo B, Anahory T, Hamamah S: The occurrence of aneuploidy in human: lessons from the cytogenetic studies of human oocytes. *Eur J Med Genet* 2006; **49**: 103–116.
23 Sloter E, Nath J, Eskenazi B, Wyrobek AJ: Effects of male age on the frequencies of germinal and heritable chromosomal abnormalities in humans and rodents. *Fertil Steril* 2004; **81**: 925–943.
24 Kotzot D: Advanced parental age in maternal uniparental disomy (UPD): implications for the mechanism of formation. *Eur J Hum Genet* 2004; **12**: 343–346.
25 Fokstuen S, Ginsburg C, Zachmann M, Schinzel A: Maternal uniparental disomy 14 as a cause of intrauterine growth retardation and early onset of puberty. *J Pediatr* 1999; **134**: 689–695.
26 Hordijk R, Wierenga H, Scheffer H, Leegte B, Hofstra RM, Stolte-Dijkstra I: Maternal uniparental disomy for chromosome 14 in a boy with a normal karyotype. *J Med Genet* 1999; **36**: 782–785.
27 Sanlaville D, Aubry MC, Dumez Y *et al*: Maternal uniparental heterodisomy of chromosome 14: chromosomal mechanism and clinical follow up. *J Med Genet* 2000; **37**: 525–528.
28 Towner DR, Shaffer LG, Yang SP, Walgenbach DD: Confined placental mosaicism for trisomy 14 and maternal uniparental disomy in association with elevated second trimester maternal serum human chorionic gonadotrophin and third trimester fetal growth restriction. *Prenat Diagn* 2001; **21**: 395–398.
29 Aretz S, Raff R, Woelfle J *et al*: Maternal uniparental disomy 14 in a 15-year-old boy with normal karyotype and no evidence of precocious puberty. *Am J Med Genet A* 2005; **135**: 336–338.
30 Mitter D, Buiting K, von Eggeling F *et al*: Is there a higher incidence of maternal uniparental disomy 14 [upd(14)mat]? Detection of 10 new patients by methylation-specific PCR. *Am J Med Genet A* 2006; **140**: 2039–2049.

Supplementary Information accompanies the paper on European Journal of Human Genetics website (http://www.nature.com/ejhg)

RESEARCH LETTER

AMERICAN JOURNAL OF medical genetics PART A

FOP in China and Japan: An Overview From Domestic Literatures

Shuang Jiao,[1] Yasu Zhang,[1] Wenhao Ma,[2] and Nobuhiko Haga[1]*

[1]Department of Rehabilitation Medicine, Graduate School of Medicine, The University of Tokyo, Hongo, Bunkyo-ku, Tokyo, Japan

[2]School of Acupuncture Moxibustion and Tuina, Beijing University of Chinese Medicine, Beijing, China

Manuscript Received: 11 April 2012; Manuscript Accepted: 11 October 2012

How to Cite this Article:
Jiao S, Zhang Y, Ma W, Haga N. 2013. FOP in China and Japan: An overview from domestic literatures.
Am J Med Genet Part A 161A:892–893.

TO THE EDITOR:

FOP is an autosomal dominant disorder, characterized by progressive ectopic ossification leading to devastating physical disabilities and malformation of the great toe and occasionally of the thumb. It is known that an activating mutation of *ACVR1* is responsible for FOP. FOP is a rare disorder with incidence of 1/2,000,000 [Connor and Evans, 1982a,b]. China has a population of more than 1.3 billion, and Japan has about 0.13 billion people. Although the FOP case reports published in China and Japan might provide valuable information for this rare disease considering their large populations, most cases were published in medical journals of their own respective languages. In order to obtain the information of FOP patients reported in Chinese and Japanese, we summarized the FOP case reports published in China and Japan and analyzed the similarities and differences of the Chinese and Japanese patients to compare their characteristics with those of reports published in international journals.

Literature search was made by using relevant key words in three Chinese and one Japanese electronic databases (Fig. 1). The case reports on FOP published in Chinese or Japanese were included in this research. All references of the identified articles were screened and the relevant articles were also retrieved (see Supporting Information online). Similar case reports were confirmed by telephone to the original author and duplicate publications were excluded.

A total of 86 Chinese patients (46 males and 40 females) and 41 Japanese patients (21 males and 20 females) were included. The median age of onset was defined as the age of first flare-up leading to heterotopic ossification. The clinical information of all patients including age of onset, age of diagnosis, site of heterotopic ossification, malformation, and interventions were extracted (Table I). A total of 32% Chinese and 83% Japanese patients were reported as having spinal deformities such as scoliosis, lordosis, or kyphosis. Unfortunately, 11 Chinese and 19 Japanese patients underwent surgical intervention, but the percentage of patients who underwent surgeries decreased in recent 10 years for both Chinese and Japanese patients. Medical intervention included administration of steroid hormones, non-steroidal anti-inflammatory drugs (including cyclooxygenase-2 inhibitor drugs), and diphosphonates-EHDP.

It was reported in earlier articles that almost all FOP patients had characteristic malformations of the great toes [Connor and Evans, 1982a,b; Kitterman et al., 2005; Janati et al., 2007]. However in several recent studies, normal great toes and late onset heterotopic ossification were reported with patients with FOP variants [Bocciardi et al., 2009; Kaplan et al., 2009; Barnett et al., 2011]. The classic FOP (with the characteristic features of great toe malformations and progressive heterotopic ossification), FOP-plus (classic defining features of FOP plus one or more atypical features) and FOP variants (major variations in one or both of the two classic defining features of FOP) were reported as having different types of *ACVR1* mutation which showed correlations with the age of onset of heterotopic ossification or malformations [Kaplan et al., 2009]. In this study, 7% of the Chinese patients and 2% of the Japanese patients were reported as having normal toes. In a previous research, 59% of FOP patients were reported as having malformed thumbs [Connor and Evans, 1982a,b]. While in this study, only 21% of the Chinese and 12% of the Japanese patients were reported as having malformed thumb. Because the exact

Additional supporting information may be found in the online version of this article.

Grant sponsor: JSPS Postdoctoral Fellowship; Grant numbers: FY2010, P10714; Grant sponsor: Health and Labor Sciences Grants; Grant sponsor: Ministry of Health Labor and Welfare.

Conflict of interest: None.

Shuang Jiao and Yasu Zhang contributed equally to this work.

*Correspondence to:
Nobuhiko Haga, M.D., Ph.D., Department of Rehabilitation Medicine, Graduate School of Medicine, The University of Tokyo, 7-3-1 Hongo, Bunkyo-ku, 113-8655 Tokyo, Japan. E-mail: hagan-reh@h.u-tokyo.ac.jp

Article first published online in Wiley Online Library (wileyonlinelibrary.com): 26 February 2013
DOI 10.1002/ajmg.a.35771

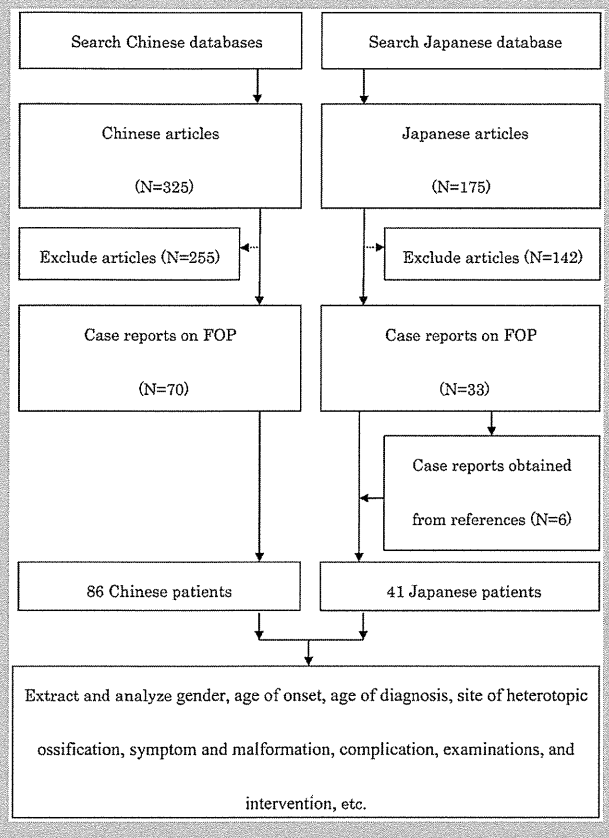

FIG. 1. Three Chinese electronic databases, including China National Knowledge Infrastructure (CNKI), Chinese Scientific Journal Databases (VIP), and Wanfang data were searched with the terms "jin xing xing gu hua xing xian wei fa yu bu liang (fibrodysplasis ossificans progressiva, FOP)" and "jin xing xing gu hua xing ji yan (myositis ossificans progressiva, MOP)" in the full text. The Japanese electronic database, Ichushi WEB, was searched with the terms "sinkousei kokkasei seniikeiseisyou (FOP)," "sinkousei kokkasei kin'en (MOP)," "sinkousei kakotusei kin'en (MOP)," "fibrodysplasis ossificans progressiva," and "myositis ossificans progressiva" in full text. After exclusion of duplicate case reports and addition of reports obtained from references, 86 Chinese and 41 Japanese patients remained for analyses.

reason for less reported percentage of malformed great toe and thumb is unknown, the ethical or racial differences of FOP subtypes and the *ACVR1* mutations with their genotype–phenotype should also be explored in future research.

Common anomalies associated with FOP such as short, broad femoral necks and metaphysical widening [Deirmengian et al., 2008] or typical complications such as baldness [Connor and Evans, 1982a,b] were not reported in these Chinese and Japanese reports. The fact may be attributed to selection-bias, because earlier reports might come from orthopedic surgeons. Lack of long-term follow up may have precluded identification of these rare onset associations.

TABLE I. Contrast of Chinese and Japanese Patients With FOP

	Chinese	Japanese
Age of onset (year): median (range)*	3.0 (0–38)	3.0 (0–16)
Age of diagnosis (year): median (range)**	10.5 (0–53)	7.0 (0–27)
Site of heterotopic ossification (%)		
At onset	Neck (30) > trunk (27) > head (13)	Neck (42) > trunk (24) > head (17)
When reported	Trunk (94) > neck (64) > shoulder (62)	Trunk (85) > neck (76) > shoulder (71)
Great toe (%): Mal/nor/no info[a]	51/7/42	73/2/24
Thumb (%): Mal/nor/no info[a]	21/9/72	12/5/83

[a]Mal/nor/no info stands for malformation/normal/no information.
*By Kolmogorov–Smirnov nonparametric test, $P = 0.532$, grand median = 3.0.
**By Kolmogorov–Smirnov nonparametric test, $P = 0.027$, grand median = 9.0.

ACKNOWLEDGMENTS

This research was supported by FY2010 JSPS Postdoctoral Fellowship for Foreign Researchers (ID No.: P10714) provided by the Japan Society for the Promotion of Science (JSPS) and the Health and Labor Sciences Grants on Intractable Diseases from the Ministry of Health, Labor, and Welfare.

REFERENCES

Barnett CP, Dugar M, Haan EA. 2011. Late-onset variant fibrodysplasia ossificans progressiva leading to misdiagnosis of ankylosing spondylitis. Am J Med Genet Part A 155A:1492–1495.

Bocciardi R, Bordo D, Di Duca M, Di Rocco M, Ravazzolo R. 2009. Mutational analysis of the ACVR1 gene in Italian patients affected with fibrodysplasia ossificans progressiva: Confirmations and advancements. Eur J Hum Genet 17:311–318.

Connor JM, Evans DA. 1982. Fibrodysplasia ossificans progressiva. The clinical features and natural history of 34 patients. J Bone Joint Surg Br 64:76–83.

Connor JM, Evans DA. 1982. Genetic aspects of fibrodysplasia ossificans progressiva. J Med Genet 19:35–39.

Deirmengian GK, Hebela NM, O'Connell M, Glaser DL, Shore EM, Kaplan FS. 2008. Proximal tibial osteochondromas in patients with fibrodysplasia ossificans progressiva. J Bone Joint Surg Am 90:366–374.

Janati J, Aghighi Y, Tofighi A, Akhavan A, Behrouzan O. 2007. Radiologic findings in seven patients with fibrodysplasia ossificans progressiva. Arch Iran Med 10:88–90.

Kaplan FS, Xu M, Seemann P, Connor JM, Glaser DL, Carroll L, Delai P, Fastnacht-Urban E, Forman SJ, Gillessen-Kaesbach G, Hoover-Fong J, Köster B, Pauli RM, Reardon W, Zaidi SA, Zasloff M, Morhart R, Mundlos S, Groppe J, Shore EM. 2009. Classical and atypical FOP phenotypes are caused by mutations in the BMP type I receptor ACVR1. Hum Mutat 30:379–390.

Kitterman JA, Kantanie S, Rocke DM, Kaplan FS. 2005. Iatrogenic harm caused by diagnostic errors in fibrodysplasia ossificans progressiva. Pediatrics 116:654–661.

Journal of Human Genetics (2013), 1–4

www.nature.com/jhg

SHORT COMMUNICATION

Exome sequencing identifies a novel *INPPL1* mutation in opsismodysplasia

Aritoshi Iida[1,9], Nobuhiko Okamoto[2,9], Noriko Miyake[3,9], Gen Nishimura[4], Satoshi Minami[5], Takuya Sugimoto[6], Mitsuko Nakashima[3], Yoshinori Tsurusaki[3], Hirotomo Saitsu[3], Masaaki Shiina[7], Kazuhiro Ogata[7], Shigehiko Watanabe[8], Hirofumi Ohashi[8], Naomichi Matsumoto[3] and Shiro Ikegawa[1]

Opsismodysplasia is an autosomal recessive skeletal disorder characterized by facial dysmorphism, micromelia, platyspondyly and retarded bone maturation. Recently, mutations in the gene encoding inositol polyphosphate phosphatase-like 1 (INPPL1) are found in several families with opsismodysplasia by a homozygosity mapping, followed by whole genome sequencing. We performed an exome sequencing in two unrelated Japanese families with opsismodysplasia and identified a novel *INPPL1* mutation, c.1960_1962delGAG, in one family. The mutation is predicted to result in an in-frame deletion (p.E654del) within the central catalytic 5-phosphate domain. Our results further support that *INPPL1* is the disease gene for opsismodysplasia and that opsismodysplasia has genetic heterogeneity.
Journal of Human Genetics advance online publication, 4 April 2013; doi:10.1038/jhg.2013.25

Keywords: exome sequencing; INPPL1; opsismodysplasia

INTRODUCTION

Opsismodysplasia (OMIM 258480) is a rare skeletal dysplasia identifiable at birth. Its clinical features are rhizomelic micromelia and facial dysmorphism, including prominent brow, large fontanels, depressed nasal bridge and small anteverted nose with long philtrum, as well as short feet and hands with sausage-like fingers.[1] Its main radiological features include retarded bone maturation, marked shortness of the bones of hands and feet with concave metaphyses and thin, lamellar vertebral bodies. Some patients show severe phosphate wasting. Autosomal recessive inheritance is the most likely mode of inheritance; to date, at least three consanguineous families with opsismodysplasia are reported.[2–4]

Recently, Below *et al.*[5] performed a homozygosity mapping coupled with whole genome sequencing in a consanguineous family with opsismodysplasia, and identified *INPPL1* (inositol polyphosphate phosphatase-like 1) as a causative gene for opsismodysplasia. They first identified a homozygous missense mutation, p.Pro659Leu, in the consanguineous family, and then found *INPPL1* mutations in additional five unrelated families with opsismodysplasia. We performed a whole exome sequencing for two patients from two unrelated families and identified a homozygous in-frame deletion of *INPPL1* in one family.

SUBJECTS AND METHODS

Subjects and DNA samples

Two families with clinical diagnosis of opsismodysplaisa were included in the study. Family 1 consisted of parents and affected sibs (Figure 1a), and Family 2 consisted of parents and a patient. Genomic DNA was extracted by standard procedures from peripheral blood of the patients and their family members after informed consent. The study was approved by the ethical committee of RIKEN, Yokohama City University, and participating institutions.

Exome sequencing

Six individuals in the two families were analyzed by the whole exome sequence as described previously.[6] Briefly, 3 μg of genomic DNA was sheared by Covaris 2S system (Covaris, Woburn, MA, USA) and partitioned using SureSelect Human All Exon V4 (Agilent technology, Santa Clara, CA, USA) according to the manufacturer's instructions. The exon-enriched DNA libraries were sequenced using HiSeq2000 (Illumina, San Diego, CA, USA) with a 101-bp paired-end reads and a 7-bp index reads. Four samples (2.5 pM each, with different index) were run in one lane. HiSeq Control Software/Real-Time Analysis and CASAVA1.8.2 (Illumina) were used for image analysis and base calling. The mapping was performed to human genome hg19 using Novoalign (http://www.novocraft.com/main/page.php?s=novoalign). The aligned reads were processed by Picard to remove the polymerase chain reaction (PCR) duplicate (http://picard.sourceforge.net). The variants were called

[1]Laboratory for Bone and Joint Diseases, Center for Genomic Medicine, RIKEN, Tokyo, Japan; [2]Department of Medical Genetics, Osaka Medical Center and Research Institute for Maternal and Child Health, Osaka, Japan; [3]Department of Human Genetics, Yokohama City University Graduate School of Medicine, Yokohama, Japan; [4]Department of Pediatric Imaging, Tokyo Metropolitan Children's Medical Center, Fuchu, Japan; [5]Department of Gynecology and Obstetrics, Shingu Municipal Medical Center, Shingu, Japan; [6]Department of Pediatrics Shingu Municipal Medical Center, Shingu, Japan; [7]Department of Biochemistry, Yokohama City University Graduate School of Medicine, Yokohama, Japan and [8]Division of Medical Genetics, Saitama Children's Medical Center, Saitama, Japan
[9]These authors contributed equally to this work.
Correspondence: Professor S Ikegawa, Laboratory for Bone and Joint Diseases, Center for Genomic Medicine, RIKEN, 4-6-1 Shirokanedai, Minato-ku, Tokyo 108-8639, Japan.
E-mail: sikegawa@ims.u-tokyo.ac.jp
Received 5 January 2013; revised 6 March 2013; accepted 9 March 2013

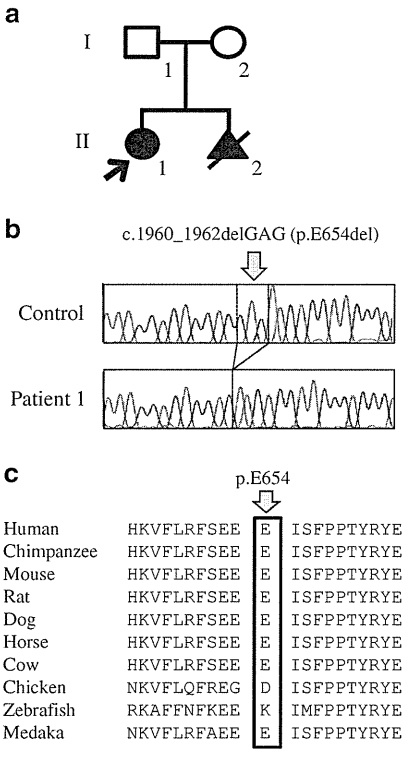

Figure 1 *INPPL1* mutation in a Japanese family with opsismodysplasia. (**a**) Pedigree, (**b**) an in-frame deletion c.1960_1962delGAG (p.E654del) within exon 17 and (**c**) conservation of p.E654 in INPPL1 among different species.

by Genome Analysis Toolkit 1.6-5 (GATK; http://www.broadinstitute.org/gsa/wiki/index.php/Main_Page) with the best practice variant detection with the GAKT v.3 (http://www.broadinstitute.org/gsa/wiki/index.php/Best_Practice_Variant_Detection_with_the_GATK_v3) and annotated by ANNOVAR (23 February 2012) (http://www.openbioinformatics.org/annovar/). Through this flow, common variants registered in dbSNP135 (minor allele frequeny $\geqslant 0.01$) (http://genome.ucsc.edu/cgi-bin/hgTrackUi?hgsid=316787363&g=snp135Common&hgTracksConfigPage=configure) were removed.

Priority scheme

On the basis of the hypothesis that opsismodysplasia is inherited in an autosomal recessive manner, variants were filtered by following conditions using the script created by BITS (Tokyo, Japan). For the homozygous mutation model: (1) variant allele frequency (variant alleles/total alleles) in probands $\geqslant 0.8$, (2) variant allele frequency in parents $\leqslant 0.8$, (3) excluding synonymous changes and (4) excluding the variants observed in our in-house database ($n = 429$). For the compound heterozygous mutation model: (1) mutation allele frequency in probands: 0.2–0.8, (2) variant allele frequency in parents $\leqslant 0.8$, (3) excluding synonymous changes, (4) excluding the variants observed in our in-house database ($n = 429$) and (5) selecting genes with compound heterozygous change. After combining variants selected by both models, genes commonly found in the two families were searched.

Sanger sequencing

We performed Sanger sequencing to confirm the deletion identified in the proband of Family 1 by the exome sequencing. We amplified exon 17 by PCR using primer sequences, 5′-AAGCACAAGGTCTTCCTTCGATTCA-3′ and 5′-CCATACCCTTGACCCAAATTCTTGAT-3′. We directly sequenced the PCR product using an Applied Biosystems 3730xl DNA analyzer (Life Technologies, Forster City, CA, USA). For the patient in Family 2, we screened 28 exons of *INPPL1* and exon–intron boundaries by direct sequencing of PCR products from genome DNA. The primer sequences are available on request.

Evaluation of polymorphism

We used the invader assay coupled with PCR[7] to exclude the possibility of polymorphism in 188 Japanese general populations. The deletion was evaluated by databases, PROVEAN v.1.1 (http://provean.jcvi.org/genome_submit.php), dbSNP (http://www.ncbi.nlm.nih.gov/projects/SNP/) and 1000 genomes (http://www.1000genomes.org/). We used Evola website to investigate the conservation of p.E654 of INPPL1 (http://www.h-invitational.jp/hinv/ahg-db/index.jsp).

RESULTS

Exome sequencing

By the whole exome sequencing, 3.8–5.1 Gb sequences uniquely mapped to all human RefSeq coding region were obtained. For all subjects, at least 95.9% of all coding regions were covered in five reads depth and more (Supplementary Table 1). No candidate genes that had mutations in the two families were identified.

Because *INPPL1* mutations have recently been identified in opsismodysplasia,[5] we checked *INPPL1* mutations in the exome sequence data. Five or more reads covered 100% of its coding regions (Supplementary Table 1). A homozygous deletion, c.1960_1962 (p.E654del), was found in the proband of Family 1 (Figure 1a). However, this deletion had been excluded as a candidate mutation because no *INPPL1* variant likely to be a mutation was detected in Family 2.

Confirmation and evaluation of c.1960_1962delGAG

We confirmed the deletion by direct sequence of PCR product from genomic DNA in the proband of Family 1 (Figure 1b). Next, we performed the invader assay coupled with PCR in the family. The parents were compound heterozygous for the deletion and the affected sibs were homozygous for it. The deletion was not found in 188 Japanese controls and in the public databases. The E654 is conserved between different species (Figure 1c). It is within the central catalytic 5-phosphate domain, but located at the position far from active site (25 amino acids) and within a loop region, which is thought to have structural flexibility in general. Inositol polyphosphate 5-phosphatase domain (ipp5c) of yeast synaptojanin in complex with inositol (1,4)-bisphosphate and calcium ion (PDB ID 1i9z) is the most analogous structure to the human INPPL1 catalytic domain among the currently available structures; however, its sequence identity with the human INPPL1 catalytic domain is low (26%). These make the structural assessment of the mutation equivocal. The PROVEAN database showed that p.E654del had a deleterious function against the gene product (score: −12.1).

Mutation screening of *INPPL1* in Family 2

We screened the *INPPL1* mutation in the patient of Family 2 by direct sequencing of the entire coding exons and their flanking regions. A total of nine SNPs were found, but no mutation was found in the patient.

Clinical information of the patients with the *INPPL1* mutation

The proband of Family 1 (II-1 in Figure 1a) was a 9-year-old girl born to non-consanguineous healthy parents. Family history was unremarkable. She was referred to one of us because fetal echogram revealed short extremities. She was born at 40 weeks' of gestation. Her birth weight was 2119 g (<3 percentile), length 38.0 cm (<3 percentile) and head circumference 35.1 cm (<3 percentile). She had a wide fontanelle, widely patent sutures, frontal bossing, flat nasal

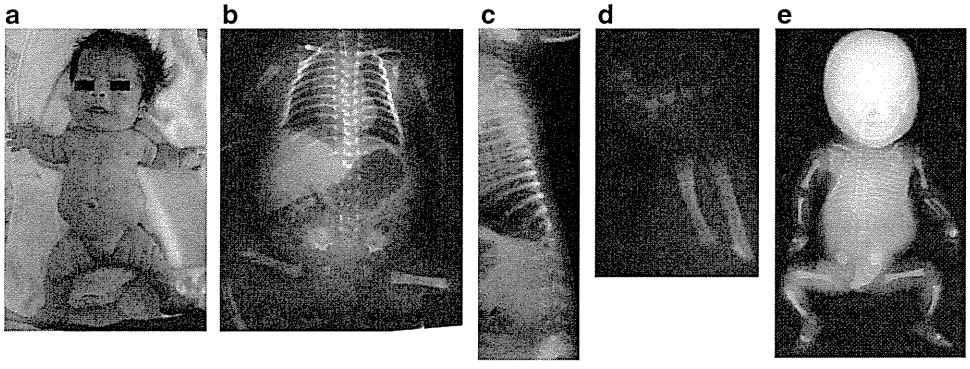

Figure 2 Phenotype of patients in Family 1. (**a**) Appearance of the proband in Family 1. Rhizomelic micromelia, frontal bossing, flat nasal bridge, low set ears, anteverted nostrils, micrognathia, narrow thorax and distended abdomen were noted. Radiographs of the proband (II-1) at birth (**b–d**) and the aborted fetus (II-2) (**e**). Characteristics of opsismodysplasia including retarded bone maturation, shortness of the bones of hands and feet, concave metaphyses and thin, lamellar vertebral bodies were noted.

bridge, low set ears, anteverted nostrils, micrognathia, narrow thorax and distended abdomen, and her extremities were remarkably short (Figure 2a). Her respiratory activity was weak and inspiratory wheezing was noted. Tracheal intubation became necessary 4 h after birth. Radiological investigations of her skeleton showed characteristics of opsisimodysplasia (Figures 2b–d). She was repeatedly admitted because of respiratory insufficiency due to infections. At 2 years of age, tracheotomy was performed to care for respiratory problems. She was noticed to show low serum phosphate levels at around 1 year and since then had been treated on phosphate supplements and/or alfacalcidol (1α-OH-D_3). At age 9 years, her height was 65 cm (<−6 s.d.) and weight 9 kg (−4 s.d). Her intellectual development was normal and was attending an elementary school.

In the second pregnancy, similar conditions were found by a fetal echogram. Artificial abortion was carried out. The post-mortem radiograph showed skeletal findings similar to the proband (Figure 2e).

DISCUSSION

Below *et al.*[5] examined *INPPL1* in a total of 12 unrelated families with opsismodysplasia and found its mutations in seven families. The list of mutation includes missense, nonsense and splicing mutations; all are predicted to be loss of function mutations. In one family, we also found a deletion mutation in *INPPL1* that is predicted to be a loss of function mutation, but in another family, we could not detect an *INPPL1* mutation. These results further support the results of the previous study that *INPPL1* is the disease gene for opsismodysplasia and that opsismodysplasia has genetic heterogeneity.[5] In retrospect, the patient of Family 2 showed significant platyspondyly, yet some of the radiographic features for opsismodysplasia that include hypoplasia of the base of the skull on lateral views and lateral spikes of the acetabular roof were absent. Further, the fragmented epiphyses and coning of the distal femora are not characteristically seen in opsismodysplasia. This case is also different from the other cases with an opsismodysplasia phenotype that do not have *INPPL1* mutations (Prof. Debora Krakow, personal communication). Further collection of *INPPL1* mutation-proven cases would help in defining the phenotype of opsismodysplasia. While we were preparing the manuscript, another study reporting the identification of *INPPL1* as the cause of opsismodysplasia was published.[8] It reports identification of the *INPPL1* mutation in all 10 families examined.

INPPL1 (also known as SHIP2) is a member of the inositol 5′-phosphatase family that hydrolyzes phosphatidylinositol 3,4,5-triphosphate (PtdIns(3,4,5)P_3) and generates phosphatidylinositol 3,4-bisphosphate (PtdIns(3,4)P_2).[9] *INPPL1* encodes a 142-kDa protein with a variety of protein interaction domains, including an N-terminal SH2 domain, a central catalytic 5-phosphatase domain, a C-terminal proline-rich domain, an NPXY site and a sterile a motif domain in the C-terminal region.[10] At least 12 proteins of binding partners for INPLL1, such as Shc, APS, filamin and EphA2, have been identified.[10] The genes for these binding partners are good candidates for the disease gene for the opsismodysplasia-like phenotype.

Biological roles of INPPL1 remain unclear. *INPPL1* expression is particularly high in heart, skeletal muscle and placenta.[11,12] Its proposed roles are cell adhesion and spreading, actin cytoskeletal remodeling and receptor internalization. INPPL1 negatively regulates insulin signaling through its catalytic PtdIns(3,4,5) P_3 5-phosphatase activity.[9] The *INPPL1*$^{-/-}$ mice show a shortened snout and grow more slowly than wild-type littermates.[13] After 6 weeks of age, they showed a substantial reduced body length and body weight; however, radiographic analysis showed no gross skeletal deficit. Further studies are necessary to clarify the role of *INPPL1* in skeletal development and homeostasis.

ACKNOWLEDGEMENTS

We thank the patients and their family for their help to the study. We also thank the Japanese Skeletal Dysplasia Consortium. This study is supported by research grants from the Ministry of Health, Labor and Welfare (23300101 to SI and NMat.; 23300201 to SI), by Grants-in-Aid for Young Scientists (23689052 to NMiy.) from the Japan Society for the Promotion of Science; by Research on intractable diseases, Health and Labour Sciences Research Grants, H23-Nanchi-Ippan-123 (SI) and by grants from the Japan Science and Technology Agency, the Strategic Research Program for Brain Sciences (11105137 to NMat.), a Grant-in-Aid for Scientific Research on Innovative Areas (Transcription Cycle) from the Ministry of Education, Culture, Sports, Science and Technology of Japan (12024421 to NMat.), a Grant-in-Aid for Scientific Research from the Japan Society for the Promotion of Science (12020465 to NMat.) and the Takeda Science Foundation (to N Miy. and N Mat.). We thank Professors Debora Krakow and Michael Bamshad for their comments on the patients' phenotypes. We also thank Ms Tomoko Kusadokoro for technical assistance.

1 Cormier-Daire, V., Delezoide, A. L., Philip, N., Marcorelles, P., Casas, K., Hillion, Y. *et al.* Clinical, radiological, and chondro-osseous findings in opsismodysplasia: survey of a series of 12 unreported cases. *J. Med. Genet.* **40,** 195–200 (2003).
2 Beemer, F. A. & Kozlowski, K. S Additional case of opsismodysplasia supporting autosomal recessive inheritance. *Am. J. Med. Genet.* **49,** 344–347 (1994).
3 Santos, H. G. & Saraiva, J. M Opsismodysplasia: another case and literature review. *Clin. Dysmorphol.* **4,** 222–226 (1995).
4 Tyler, K., Sarioglu, N. & Kunze, J Five familial cases of opsismodysplasia substantiate the hypothesis of autosomal recessive inheritance. *Am. J. Med. Genet.* **83,** 47–52 (1999).
5 Below, J. E., Earl, D. L., Shively, K. M., McMillin, M. J., Smith, J. D., Turner, E. H. *et al.* Whole-genome analysis reveals that mutations in inositol polyphosphate phosphatase-like 1 cause opsismodysplasia. *Am. J. Hum. Genet.* **92,** 137–143 (2013).
6 Miyake, N., Elcioglu, N. H., Iida, A., Isguven, P., Dai, J., Murakami, N. *et al.* PAPSS2 mutations cause autosomal recessive brachyolmia. *J. Med. Genet.* **49,** 533–538 (2012).
7 Ohnishi, Y., Tanaka, T., Ozaki, K., Yamada, R., Suzuki, H. & Nakamura, Y A high-throughput SNP typing system for genome-wide association studies. *J. Hum. Genet.* **46,** 471–477 (2001).
8 Huber, C., Faqeih, E. A., Bartholdi, D., Bole-Feysot, C., Borochowitz, Z., Cavalcanti, D. P. *et al.* Exome sequencing identifies INPPL1 mutations as a cause of opsismodysplasia. *Am. J. Hum. Genet.* **92,** 144–149 (2013).
9 Dyson, J. M., Kong, A. M., Wiradjaja, F., Astle, M. V., Gurung, R. & Mitchell, C. A The SH2 domain containing inositol polyphosphate 5-phosphatase-2: SHIP2. *Int. J. Biochem. Cell. Biol.* **37,** 2260–2265 (2005).
10 Suwa, A., Kurama, T. & Shimokawa, T. SHIP2 and its involvement in various diseases. *Expert Opin. Ther. Targets* **14,** 727–737 (2010).
11 Hejna, J. A., Saito, H., Merkens, L. S., Tittle, T. V., Jakobs, P. M., Whitney, M. A. *et al.* Cloning and characterization of a human cDNA (INPPL1) sharing homology with inositol polyphosphate phosphatases. *Genomics* **29,** 285–287 (1995).
12 Pesesse, X., Deleu, S., De Smedt, F., Drayer, L. & Erneux, C Identification of a second SH2-domain-containing protein closely related to the phosphatidylinositol polyphosphate 5-phosphatase SHIP. *Biochem. Biophys. Res. Commun.* **239,** 697–700 (1997).
13 Sleeman, M. W., Wortley, K. E., Lai, K. M., Gowen, L. C., Kintner, J., Kline, W. O. *et al.* Absence of the lipid phosphatase SHIP2 confers resistance to dietary obesity. *Nat. Med.* **11,** 199–205 (2005).

Supplementary Information accompanies the paper on Journal of Human Genetics website (http://www.nature.com/jhg)

ORIGINAL ARTICLE

PAPSS2 mutations cause autosomal recessive brachyolmia

Noriko Miyake,[1] Nursel H Elcioglu,[2] Aritoshi Iida,[3] Pinar Isguven,[4] Jin Dai,[3] Nobuyuki Murakami,[5] Kazuyuki Takamura,[6] Tae-Joon Cho,[7] Ok-Hwa Kim,[8] Tomonobu Hasegawa,[9] Toshiro Nagai,[5] Hirofumi Ohashi,[10] Gen Nishimura,[11] Naomichi Matsumoto,[1] Shiro Ikegawa[3]

[1]Department of Human Genetics, Yokohama City University Graduate School of Medicine, Yokohama, Japan
[2]Department of Pediatric Genetics, Marmara University Pendik Hospital, Istanbul, Turkey
[3]Laboratory for Bone and Joint Diseases, Center for Genomic Medicine, RIKEN, Tokyo, Japan
[4]Department of Pediatrics and Pediatric Endocrinology, Medeniyet University Goztepe Hospital, Istanbul, Turkey
[5]Department of Pediatrics, Dokkyo Medical University Koshigaya Hospital, Koshigaya, Japan
[6]Department of Orthopaedic Surgery, Fukuoka Children's Hospital, Fukuoka, Japan
[7]Division of Pediatric Orthopaedics, Seoul National University Children's Hospital, Seoul, Korea
[8]Department of Radiology, Ajou University Hospital, Suwon, Korea
[9]Department of Pediatrics, Keio University School of Medicine, Tokyo, Japan
[10]Division of Medical Genetics, Saitama Children's Medical Center, Saitama, Japan
[11]Department of Pediatric Imaging, Tokyo Metropolitan Children's Medical Center, Futyu, Japan

Correspondence to
Noriko Miyake, Department of Human Genetics, Yokohama City University Graduate School of Medicine, 3-9, Fukuura, Kanazawa-ku, Yokohama 236-0004, Japan; nmiyake@yokohama-cu.ac.jp or Shiro Ikegawa, Laboratory of Bone and Joint Diseases, Center for Genomic Medicine, RIKEN 4-6-1 Shirokanedai, Minato-ku, Tokyo 108-8639, Japan; sikegawa@ims.u-tokyo.ac.jp

NM, NHE and AI contributed equally to this work.

Received 8 May 2012
Revised 8 June 2012
Accepted 10 June 2012

ABSTRACT

Background Brachyolmia is a heterogeneous group of skeletal dysplasias that primarily affects the spine. Clinical and genetic heterogeneity have been reported; at least three types of brachyolmia are known. *TRPV4* mutations have been identified in an autosomal dominant form of brachyolmia; however, disease genes for autosomal recessive (AR) forms remain totally unknown. We conducted a study on a Turkish family with an AR brachyolmia, with the aim of identifying a disease gene for AR brachyolmia.

Methods and results We examined three affected individuals of the family using exon capture followed by next generation sequencing and identified its disease gene, *PAPSS2* (phosphoadenosine-phosphosulfate synthetase 2). The patients had a homozygous loss of function mutation, c.337_338insG (p.A113GfsX18). We further examined three patients with similar brachyolmia phenotypes (two Japanese and a Korean) and also identified loss of function mutations in *PAPSS2*; one patient was homozygous for IVS3+2delT, and the other two were compound heterozygotes for c.616-634del19 (p.V206SfsX9) and c.1309-1310delAG (p.R437GfsX19), and c.480_481insCGTA (p.K161RfsX6) and c.661delA (p.I221SfsX40), respectively. The six patients had short-trunk short stature that became conspicuous during childhood with normal intelligence and facies. Their radiographic features included rectangular vertebral bodies with irregular endplates and narrow intervertebral discs, precocious calcification of rib cartilages, short femoral neck, and mildly shortened metacarpals. Spinal changes were very similar among the six patients; however, epiphyseal and metaphyseal changes of the tubular bones were variable.

Conclusions We identified *PAPSS2* as the disease gene for an AR brachyolmia. *PAPSS2* mutations have produced a skeletal dysplasia family, with a gradation of phenotypes ranging from brachyolmia to spondylo-epi-metaphyseal dysplasia.

INTRODUCTION

Brachyolmia is a heterogeneous group of skeletal dysplasias that primarily affects the spine. The name comes from the Greek for 'short trunk'; patients with brachyolmia have short stature due to a short trunk.[1] Conceptually, skeletal lesions of brachyolmia are limited to the spine; however, it is generally thought that pure brachyolmia (spine-only dysplasia) does not exist and that metaphyseal and/or epiphyseal involvements may be minimal and scattered, but are always present along with spinal involvements in cases labelled brachyolmia.[2]

Clinical and genetic heterogeneity have been reported in brachyolmia. At least three relatively well defined types of brachyolmia are known: type 1 that includes the Hobaek (OMIM 271530) and Toledo (OMIM 271630) forms; type 2 (OMIM 613678) referred to as the Maroteaux type; and type 3 (OMIM 113500). The former two types are autosomal recessive (AR) traits, while the latter is an autosomal dominant trait. Type 1 is characterised by scoliosis, platyspondyly with rectangular and elongated vertebral bodies, overfaced pedicles, and irregular and narrow intervertebral spaces. The Toledo form is distinguished from the Hobaek form by the presence of corneal opacity and precocious calcification of the costal cartilage.[3 4] Type 2 is distinguished by rounded vertebral bodies, less overfaced pedicles, minor facial anomalies, and precocious calcification of the falx cerebri.[1] Type 3 is characterised by severe kyphoscoliosis and flattened, irregular cervical vertebrae. Heterozygous mutations in the *TRPV4* (transient receptor potential vanilloid 4) gene (OMIM 605427) have been identified in several patients with type 3, autosomal dominant brachyolmia;[5 6] however, disease genes for recessive forms of brachyolmia remain totally unknown.

To identify novel disease genes from a limited number of subjects, exome sequencing (exon capture followed by next generation sequencing) is a promising approach. This approach sometimes presents us with unusual and unexpected connection between genes and phenotypes, thereby opening a new window for biology and medicine. We experienced a family with an AR form of brachyolmia harbouring three affected individuals. By performing exome sequencing for the family, we have identified the disease gene for the recessive brachyolmia, *PAPSS2* (phosphoadenosine-phosphosulfate synthetase 2). The discovery was confirmed by identification of *PAPSS2* mutations in three sporadic patients with different ethnic backgrounds but similar brachyolmia phenotypes. All patients had loss of function mutations of *PAPSS2* in both chromosomes.

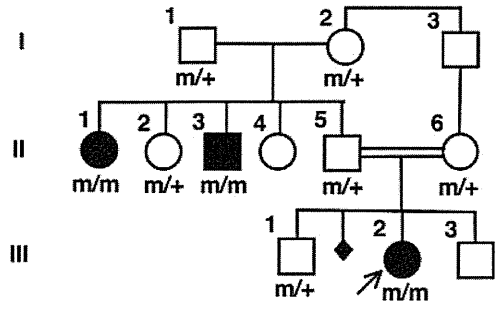

Figure 1 The pedigree of family 1 and co-segregation of the *PAPSS2* mutation (c.337_338insG) in the family. m: mutation allele, +: wild type allele.

MATERIALS AND METHODS

Subjects

P1-3 (family 1)

The proband (P1; III-2 in figure 1) was a Turkish girl referred to one of us (NHE) for genetic evaluation at the age of 8 years 4 months. She has been followed up for her spinal deformity and lumber pain elsewhere for 5 years. She was the result of a consanguineous (first cousin) marriage. A paternal uncle (P2; II-3 in figure 1) and aunt (P3; II-1 in figure 1) had the similar disease (table 1). The paternal grandparents originated from a small area and could be related. The inheritance of the disease was consistent with AR mode. Her birth length was 49 cm and weight 2800 g. She did not gain well after birth and was investigated for short stature at the age of 1 year. Her back deformity was noticed at around 3 years of age. On examination, she had short-trunk short stature. Her height was 109 cm (−3.2 SD), weight 29 kg (+0.38 SD) and head circumference 51 cm (−0.6 SD). She was mentally normal with no hearing or vision problems. She had widened wrists, bulbous proximal interphalangeal joints, clinodactyly of the fifth finger, and bowing deformity in her left lower leg. Serum DHEA-S (dehydroepiandrosterone-sulfate) was under the detection limit (<15.0 μg/dl).

Repeated skeletal surveys showed definite spondylodysplasia with minimal epiphyseal and metaphyseal changes, which was compatible with brachyolmia (table 1 and figure 2). Vertebral bodies were flat, particularly in thoracic spines. Endplates were irregular and intervertebral disc spaces were narrowed. The acetabular roof was horizontal. Femoral necks were slightly short. Metaphyses of the distal tibias had striation. Metacarpals were mildly shortened with mild metaphyseal changes. The bone age was advanced; 6 years 10 months at chronological age 5 years 8 months, and 10 years at chronological age 8 years 2 months (Greulich-Pyle method). MRIs and CTs showed no calcification of the falx cerebri.

At her last visit (10 years 4 months old), she had increasing back deformity and pain. Her height was 121 cm (−3.4 SD), arm span 119 cm, and sitting/standing height ratio was 0.53.

Table 1 Clinical and radiographic phenotypes of autosomal recessive brachyolmina harbouring *PAPSS2* mutation (in comparison to those in spondylo-epi-metaphyseal dysplasia Pakistani type)

Patient ID	P1	P2	P3	P4	P5	P6	
Family	Family 1						Patient reported by Noordam *et al*
Intra-family ID	III-2	II-3	II-1	Family 2	Family 3	Family 4	
Country of origin	Turkey			Japan	Japan	Korea	Turkey
Sex	Female	Male	Female	Female	Female	Male	Female
Age at first presentation	8 years 4 months	29 years	40 years	11 years 4 months	8 years 8 months	12 years 7 months	8 years
Birth length (cm)	49	NA	NA	46	47	50	NA
Birth weight (g)	2800	NA	NA	3340	2676	3100	NA
Consanguinity of the parents	+	Probably +	Probably +	(−)	(−)	(−)	(−)
Clinical feature							
Normal intelligence	+	+	+	+	+	+	NA
Normal facies	+	+	+	+	+	+	NA
Short-trunk short stature	+	+	+	+	+	+	+
Spinal deformity	Kyphosis	(−)	Kyphosis, lumbar scoliosis	Kyphosis	(−)	(−)	Lumbar scoliosis
Leg deformity	Bil genu varum and internal rotation	(−)	Bil genu varum and internal rotation	(−)	Right genu valgum	Bil genu varum	NA
Androgen excess sign	(−)	(−)	(−)	(−)	(−)	(−)	+
Radiographic feature							
Rectangular vertebra	+	+	+	+	+	+	+
Irregular endplate	+	+	+	+	+	+	+
Narrowed disc	+	+	+	+	+	+	+
Precocious calcification of costal cartilage	(−)	+	+	+	(−)	(−)	NA
Delayed ossification of hip and knee epiphyses	(−)	NA	NA	(−)	(−)	(−)	(−)
Early osteoarthritic change	(−)*	(−)	(−)	(−)	(−)*	(−)*	(−)*
Short femoral neck	+	+	+	+	+	+	+
Metaphyseal abnormality†	Dist tibia	Prox tibia	Prox tibia	(−)	(−)	Prox tibia	(−)
Mild brachymetacarpia	+	+	+	+	+	+	+
Advanced bone age	+	NA	NA	+	+	+	+

*May be too young to be evaluated.
†Other than short femoral neck and fingers.
Bil, bilateral; Dist, distal; NA, not available or assessed; Prox, proximal.

J Med Genet 2012;**49**:533–538. doi:10.1136/jmedgenet-2012-101039

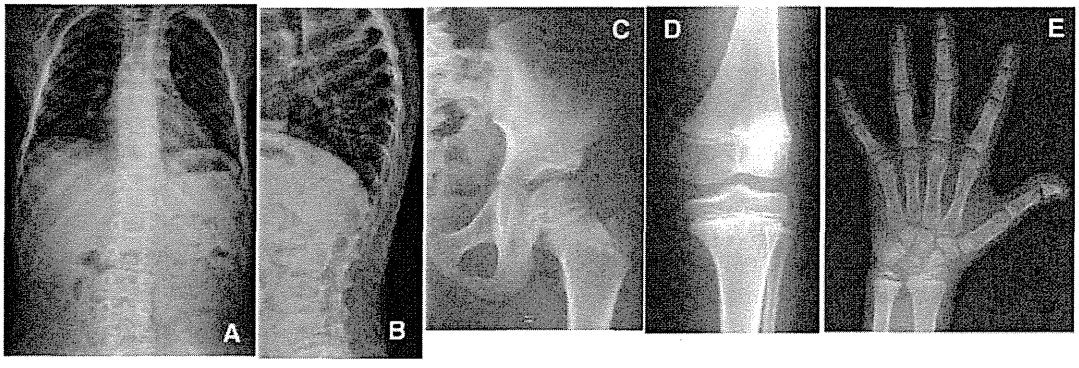

Figure 2 Radiographs of P1 (III-2 in family 1) at age 8.5 years. (A) Spine anteroposterior (AP). Mildly overfaced vertebra. (B) Lateral spine. Mild flattening of vertebral bodies and irregular endplates. (C) Left hip AP. Almost normal epiphysis. (D) Left knee AP. Epiphyseal and metaphyseal abnormalities are unremarkable. (E) Left hand AP. Metacarpals are mildly shortened with mild irregularity of the growth plates. Epiphyses of the distal radius and ulna show mild dysplasia. The bone age is advanced.

Breast development was Tanner 2–3, pubic hair Tanner 1. There had been no sign of androgen excess (acne, hirsutism, etc).

P4-6 (sporadic cases)

After we found *PAPSS2* mutations in family 1, we reviewed the patient registry of the Japanese Skeletal Dysplasia Consortium and found two Japanese patients (P4-5) and one Korean patient (P6) who had similar phenotypes to those of the Turkish family (table 1 and figure 3); all three were sporadic cases from normal, non-consanguineous parents and were *TRPV4* mutation negative.

DNA sample

Genomic DNA was extracted by standard procedures from peripheral blood of the patients and/or their family members after informed consent. The study was approved by the ethical committee of RIKEN, Yokohama City University, and participating institutions.

Exome sequencing

Three affected individuals of family 1 (II-1, II-3 and III-2) were analysed by whole exome sequencing as previously reported (see supplementary online table S1).[7 8] In brief, 3 μg of genomic DNA was sheared by Covaris S2 system (Covaris, Woburn, Massachusetts, USA) and processed using a SureSelect Human All Exon 50 Mb Kit (Agilent Technologies, Santa Clara, California, USA) according to the manufacturer's instructions. DNAs were captured by the kit and were sequenced by GAIIx (Illumina, San Diego, California, USA) with 108 pair-ends reads. Each sample was run in one lane. Image analysis and base calling were performed by sequence control software 2.9 and real time analysis 1.9 (Illumina), and CASAVA software V.1.8.1 (Illumina). The quality-controlled (path-filtered) reads were mapped to human genome reference hg19 with Mapping and Assembly with Qualities (MAQ, http://maq.sourceforge.net/) and NextGENe software V.2.00 (SoftGenetics, State College, Pennsylvania, USA). The variants from MAQ were annotated by SeattleSeq annotation 131 (http://snp.gs.washington.edu/SeattleSeqAnnotation131/).

Priority scheme

Variants were filtered by the following conditions using the script created by BITS (Tokyo, Japan): (1) variants only annotated on human autosomes and chromosome X; (2) variants not in dbSNP131, dbSNP134, the 1000 Genomes database (http://www.1000genomes.org/), and in-house exome data of normal Japanese controls (n=66); (3) variants that were non-synonymous and intronic changes (±20 bp from exon/intron boundaries) called in common by NextGENe and MAQ, and variants of insertion/deletion with a NextGENe score ≥10. The variant numbers in each category are shown in supplementary online table S1.

Sanger sequencing and evaluation of mutations

To confirm the sequence change identified in P1-3 by the exome sequencing, exon 3 of *PAPSS2* and its flanking intronic sequences (The GenBank reference sequence: NM_001015880) were amplified by PCR from genomic DNA. To examine *PAPSS2* mutation in P4-6, all exons of *PAPSS2* and its flanking intronic sequences were amplified by PCR from genomic DNA. Primer sequences and PCR conditions were as previously described.[9] PCR products were directly sequenced using ABI Prism automated sequencers 3730 (PE Biosystems, Foster City, CA, USA).

To evaluate the possibility of polymorphisms, identified sequence changes were genotyped in 93 ethnically matched controls using the invader assay coupled with PCR as described previously.[10] The sequence changes were evaluated by public databases including OMIM (http://www.ncbi.nlm.nih.gov/omim) and dbSNP (http://www.ncbi.nlm.nih.gov/projects/SNP/).

RESULTS

Exome sequencing

A total of 90 964 194 (II-1), 90 508 738 (II-3) and 90 223 680 (III-2) reads were mapped to the whole human genome in pairs by MAQ. Considering the consanguinity of the family, we focused on the same homozygous mutations shared by the three affected individuals. After filtering, a total of 37 homozygous variants remained as candidates (23 missense, 11 intronic, and three insertion changes) (see supplementary online table S1). Among them, one base pair insertion, c.337_338insG in exon 3 of *PAPSS2*, was highlighted because it is a causative gene for SEMD, Pakistani type (OMIM 612847), that has overlapping features with the phenotypes of the three patients.

The insertion sequence was confirmed by direct sequence of PCR products from genomic DNA. Direct sequencing of nine family members showed co-segregation of the mutation with the disease phenotype (figure 1). The insertion mutation was